Mannoside and 1,2-mannobioside β-cyclodextrin-scaffolded NO-photodonors for targeting antibiotic resistant bacteria

Giovanna Cutrone,[a] Gábor Benkovics,[b] Milo Malanga,[b] Juan Manuel Casas-Solvas,[a] Éva Fenyvesi,[b] Salvatore Sortino,[c] Luis García-Fuentes,[a] Antonio Vargas-Berenguel[a,*]

[a] Department of Chemistry and Physics, University of Almería, Carretera de Sacramento s/n, E-04120, Almería, Spain

[b] Cyclolab Kft, Illatos út 7, H-1097, Budapest, Hungary

[c] Department of Drug Sciences, University of Catania, Viale Andrea Doria 6, I-95125, Catania, Italy

∗ Corresponding author. E-mail address: avargas@ual.es (A. Vargas-Berenguel).

ABSTRACT

Two β-cyclodextrin derivatives randomly appended on the primary face with both the nitric oxide (NO) photodonor 4-nitro-3-(trifluoromethyl)aniline and a mannose or α(1→2)mannobioside residue are reported to construct targeted NO photoreleasing nanocarriers. 2D ROESY and PGSE NMR suggested supramolecular homodimerization in water by inclusion of the nitroaniline group into the facing macrocycle cavities. Isothermal titration calorimetry on their concanavalin A lectin binding showed an exothermic binding event to the lectin and an endothermic process during the dilution of the conjugates. Both α(1→2)mannobioside and the nitroaniline moieties significantly enhanced the binding to the lectin. These effects might arise from a better fit within the carbohydrate-recognition site in the former case and a multivalent effect caused by homodimerization in the latter. Direct detection of NO by amperometric technique shows that both β-cyclodextrin derivatives release this radical upon excitation with visible light with higher efficiency than the unfunctionalized NO photodonor.

KEYWORDS

β-Cyclodextrin; α(1→2)Mannobioside; Homodimerization; Concanavalin A; Nitric Oxide

1. Introduction

The emergence of pathogenic bacteria that show resistance to diverse antimicrobial active ingredients is a growing global health threat (Magiorakos et al., 2012). Commonly used antimicrobial therapies, such as the administration of antibiotic drugs, fail in providing an efficient treatment due to the ability of bacteria to develop resistance mechanisms to the action of such drugs (Woodford, 2005). Thus, biomedicine faces the demanding challenge of developing new treatment strategies against antibiotic Multi Drug Resistance (MDR) (Cohen, 2000; Laxminarayan et al., 2013; Taubes, 2008). In this regard, a very promising approach is based on the use of nitric oxide (NO) as a very efficient non-conventional antimicrobial and antioxidant. As well, this inorganic free radical has a key therapeutic role in a number of cancer and cardiovascular diseases (Carpenter & Schoenfisch, 2012; Halpenny & Mascharak, 2010). The NO radical presents a mechanism of action that avoids MDR problems, as it is considered a multitarget cytotoxic agent that is able to attack a

wide range of biological targets (Szakács, Paterson, Ludwig, Booth-Gent, & Gottesman, 2006). However, delivering gaseous NO to selected targets is a difficult challenge that has fostered the development of a range of molecular NO donors (Wang et al., 2002; Wang, Cai, & Taniguchi, 2005; Riccio & Schoenfisch, 2012; Seabra & Durán, 2010). An interesting approach involves the use of biocompatible scaffolds as suitable vehicles able to release NO under light stimuli, namely NO photodonors (NOPDs). These compounds offer the great advantage to deliver NO with high spatiotemporal control, thus favoring reducing side-effects and improving therapeutic outputs (Fraix, Marino, & Sortino, 2016).

Cyclodextrins are cyclomaltooligosaccharides well known for their applications in many different fields, but particularly in the supramolecular and pharmaceutical fields. Such molecules are able to enhance the water solubility, stability, bioavailability and organoleptic properties of a large number of drugs. The doughnut-shaped structures formed by six (α-CD), seven (β-CD) and eight (γ-CD) linked glucoses, define an inner cavity of a relatively hydrophobic nature, inside of which a wide range of organic molecules of similar polarity and suitable size and shape can be hosted in aqueous media. Numerous studies carried out in humans and animals have shown that CDs can be very useful to improve drug delivery of therapeutic substances (Cutrone, Casas-Solvas, & Vargas-Berenguel, 2017; Duchêne, & Bochot, 2016; Popielec & Loftsson, 2017). The drug delivery strategy can be extended to NO therapy by the construction of photoactivatable CD-NOPD conjugates, either in covalent or non-covalent fashion, as delivery systems for the NO radical (Mazzaglia et al., 2012). Among others, 4-nitro-3-(trifluoromethyl)aniline derivatives are efficient NOPDs and suitable for bio-applications as they show dark stability and adequate absorption coefficient in the visible region, and produce NO radicals without generating toxic or light-absorbing byproducts, or altering environmental pH, temperature or ionic strength (Caruso, Petralia, Conoci, Giuffrida, & Sortino, 2007; Conoci, Petralia, & Sortino, 2006; Di Bari et al., 2016). The chromophore can enter within the cavity of β-CD, where the scarce contact with water molecules dramatically modifies both the light absorption efficiency and the mechanism of photochemical deactivation (Sortino et al., 2001). Indeed, within the hydrophobic microenvironment of a micelle, this NOPD has shown a remarkable enhancement of NO release efficiency (Di Bari et al., 2016).

The vast majority of viruses, bacteria and cells present on their surfaces a family of proteins called lectins that are able to specifically bind carbohydrates. This fact has allowed the development of drug delivery strategies based on the use of carbohydrates as selective biological vectors (Vargas-Berenguel, Ortega-Caballero, & Casas-Solvas, 2007; Casas-Solvas & Vargas-Berenguel, 2016). Thus, by conjugating a molecular carrier to carefully selected carbohydrates it is possible to transport therapeutics to those cells presenting on their surfaces the complementary saccharide receptor. In particular, oligosaccharidic mannosyl structures, such as mannobioside (α-D-Man-(1→2)-D-Man) and mannotrioside (α-D-Man-(1→2)-α-D-Man-(1→2)-D-Man), are intimately related with the pathogenicity of a good number of viruses and bacteria (Schuster, Vijayakrishnan, & Davis, 2015). For example, mannose-binding lectins (MBLs) such as FimH are displayed on the surface of many bacteria. Furthermore, cells of the immune system present a series of MBLs on their surfaces, such as macrophage-mannose receptors (MMR) on the macrophages and Dendritic Cell-Specific Intercellular adhesion molecule-3 (ICAM-3)-Grabbing Non-integrin (DC-SIGN) on the dendritic cells (Figdor, van Kooyk, & Adema, 2002). Thus, mannoside-CD conjugates able to produce antibacterial effects or to encapsulate antibacterial drugs could be used as target-specific antimicrobial delivery systems as a way to fight antibiotic resistance. However, this strategy is hindered by the intrinsic weakness of the saccharide-protein interaction, which can be overcome

through a multivalent presentation of the carbohydrate moieties to achieve a global binding potency toward the lectin higher than that for the sum of the monovalent entities (Bausanne et al., 2000; Benito et al., 2004; Vargas-Berenguel, Ortega-Caballero, & Casas-Solvas, 2007; Casas-Solvas & Vargas-Berenguel, 2016).

In this context, we describe herein the construction of photoresponsive β-CD derivatives having the CD scaffold covalently linked to the NOPD 3-(trifluoromethyl)-4-nitrobenzenamine and mannose or α(1→2)mannobioside as targeting functionalities, these latter having specific avidity for pathogens showing mannose-receptor lectins on their surface. We hypothesized that such structures would undergo a supramolecular self-aggregation process in aqueous solution through the inclusion of the NOPD within the β-CD. Such arrangement would result in a multivalent display of the carbohydrate moieties, as well as enhancing the NO-release efficiency due to the NO donor confinement inside the CD cavity. The formation of self-inclusion complexes was investigated by 2D ROESY and pulse-gradient stimulated echo (PGSE) NMR experiments, while amperometric detection allowed us to estimate the light-stimulated release of the NO radical. Isothermal titration calorimetry (ITC) served to measure the binding efficiency of these new conjugates towards Concanvalin A (ConA) lectin as a mannose-specific model protein.

2. Experimental part

2.1. Materials and methods

Merck silica gel 60 F254 aluminum sheets were used for Thin Layer Chromatography (TLC). Plates were developed by UV-Vis light and stained with 5% v/v sulfuric acid in ethanol. Merck silica gel (230-400 mesh, ASTM) was used as stationary phase for flash column chromatography. Merck Celite 545 (0.002-0.1 mm) was used for filtration when stated. Uncorrected melting points measurements were taken with a Büchi B-450 melting point equipment. Optical rotations ($[\alpha]_D$ values,(given in 10^{-1} deg cm^{-1} g^{-1}) were measured on a Jasco P-1030 polarimeter at room temperature. Attenuated Total Reflectance (ATR) infrared spectra were measured on a Bruker Alpha FTIR equipment. MALDI-TOF mass spectra using 2,5-dihydroxybenzoic acid (DHB) as matrix were recorded on a 4800 Plus AB SCIEX spectrometer, while an Agilent LC/MSD-TOF spectrometer was used to measure ESI-TOF mass spectra. Dialysis was performed using Biotech CE Tubing MWCO: 100-500 D. Absorbance UV-Vis spectra were obtained using a Jasco V 650 spectrophotometer.

D-(+)-Mannose (≥99%, Acros), acetic anhydride (purum, Panreac), $BF_3{\cdot}Et_2O$ (≥46.5% BF_3 basis, Aldrich), sodium (purum, Panreac), benzoyl chloride (99%, Aldrich), trichloroacetonitrile (98%, Aldrich), potassium carbonate (purum, Panreac), benzoyl cyanide (98%, Aldrich), trimethyl orthoacetate (99%, Aldrich), D/L-10-camphorsulfonic acid (98%, Acros), benzoic anhydride (≥95%, Aldrich), 4-dimethylaminopyridine (99%, Fluka), trimethylsilyl triflate (≥98%, Fluka), and copper(I) iodide (98%, Aldrich) were purchased from commercial sources and used without further purification otherwise indicated. β-CD (CycloLab) was dried at 50 ºC in vacuum in the presence of P_2O_5 until constant weight was achieved. 7% HCl solution in MeOH was prepared by diluting 37% aqueous HCl solution (Panreac) in distilled MeOH. Triethylenamine (≥99%, Sigma-Aldrich), pyridine (purum, Panreac), propargyl alcohol (99%, Acros), 2-aminoethanol (≥98%, Sigma-Aldrich), and organic solvents were dried according to literature procedures (Perrin & Armarego,

1989). Dry DMF (99.8%, over molecular sieves, AcroSeal) was purchased from Acros. 4Å molecular sieves (VWR Chemicals) were heated at 200 ºC under high vacuum for 12 hours for activation. 6^I-Deoxy-6^I-azido-6^X-deoxy-6^X-*N*-{3-[*N'*-(4'-nitro-3'-trifluoromethylphen-1'-yl)amino]propylamino}cyclomaltoheptaose **1** was synthesized as a mixture of regioisomers as previously reported by Benkovics et al. (2017) (see supplementary data for details). 6^I-Azido-6^I-deoxy-β-cyclodextrin **2** was purchased from CycloLab. Propargyl α-D-mannose **3** was prepared as described in literature (Poláková, Beláňová, Mikušová, Lattová, & Perreault, 2011; Zhao, Liu, Park, Boggs, & Basu, 2012) with small modifications. Specifically, purifications of both compounds after deacetylation were carried out by column chromatography using EtOAc-MeOH 6:1 as eluent. NMR data for these compounds in D_2O completely agreed those described by Erdmann & Wennermers (2010) and van der Peet et al. (2006), respectively. *O*-(2,3,4,6-tetra-*O*-benzoyl-α-D-mannopyranosyl) trichloroacetamidate **8** was prepared as described by Hartmann et al (2012).

2.2. NMR measurements

^{1}H, ^{13}C and 2D NMR spectra were recorded on a Bruker Avance III HD 600 MHz spectrometer equipped with a QCI ^{1}H/^{13}C/^{15}N/^{31}P proton-optimized quadrupole inverse cryoprobe with ^{1}H and ^{13}C cryochannels, a Bruker Avance III HD 500 MHz spectrometer equipped with an inverse TBI ^{1}H/^{31}P/BB probe, or a Bruker Nanobay Avance III HD 300 MHz spectrometer using a QNP ^{1}H/^{13}C/^{19}F/^{31}P probe, depending on the sample. Chemical shifts (δ) are given in parts per million (ppm) and *J* values are expressed in hertz (Hz). Residual solvent signals (δ_H 7.26 and δ_C 77.16 ppm for $CDCl_3$; δ_H 4.79 ppm for D_2O) were used as internal references. Water signal was suppressed in two-dimensional phase-sensitive gROESY experiments using WATERGATE 3-9-19 pulse sequence with gradients. Stimulated echo diffusion measurements (Pregosin, Kumar, & Fernandez, 2005) were performed on 10 mM samples in 500 μL of D_2O on the Bruker Avance 500 without spinning using rectangular gradient pulses of variable strength, which was increased from 10 to 98% in 8% steps) For each increment 128 scans were measured using a recovery time 5 times longer that the longest spin-lattice relaxation time (T_1) measured for each sample prior to the experiment. The slope of the linear regression on Stejskal-Tanner plots were used to determine the *D* values according to

$$\ln\left(\frac{I}{I_0}\right) = -(\gamma\delta)^2\left(\Delta - \frac{\delta}{3}\right)DG^2$$

where *I* and I_0 correspond to the signal intensity after and before applying gradients, respectively; δ is length of the gradient pulse (set to 4 ms), Δ is the delay between the midpoints of the gradients*; D* is the diffusion coefficient; and *G* is the gradient strength. Three gradient delays (Δ = 70-120 ms) were used to check the robustness of the results. Attenuation of the D_2O signal was used for calibration of the gradients, giving a slope of 1.425 x 10^{-3} when using δ = 1.75 ms and Δ = 167.75 ms). At least 7 data points were used for least-square linear fits with correlation coefficients >0.999. Obtained *D* values were estimated to have an experimental error of ±2%.

Once obtained *D* values, Stokes-Einstein equation $D = (k_B T)/(c\pi\eta r_H)$ was used to calculate the hydrodynamic radii (r_H), assuming a spherical shape for β-CD, **ManβCD** and **BiManβCD**. In this equation *D* is the diffusion coefficient, k_B is the Boltzman constant, *T* is the temperature, and η is the viscosity of the solvent (0.890 x 10^{-3} kg m^{-1} s^{-1} for H_2O as taken from www.knovel.com). Microfrictional factor *c* should be semi-empirically estimated according to ($c = 6/[1 + \{0.695(r_{solv}/r_H)^{2.234}\}]$, which take into account the ratio between the solvent and solute radii. In our

case, c can be approximated to 6 due to the fact that $r_H \geq 5r_{solv}$, as suggested by Macchioni, Ciancaleoni, Zuccaccia, & Zuccaccia, 2008. In contrast, **ManNOPDβCD** and **BiManNOPDβCD** were considered as prolate spheroids in order to take into account the potential dimerization process in water for these compounds. Their volumes were set as equal to those calculated for their equivalent spheres defined from the Stokes-Einstein equation. Their major semi-axes were then estimated assuming that their minor semi-axes could not be larger than r_H values calculated for their analogues **ManβCD** and **BiManβCD**, respectively.

2.3. NO release measurements

NO release measurements are based on short response time (< 5 s) direct amperometric detection of the radical using a World Precision Instrument, ISO-NO meter, in the sensitivity range of 1 nM-20 µM. A four-channel data acquisition system connected to a PC workstation was used to digitalize the analog signal. In order to calibrate the sensor, standard solutions of $NaNO_2$ were mixed with 0.1 M H_2SO_4 and 0.1 M KI to generate known amounts of NO according to the reaction:

$$4H^+ + 2I^- + 2NO_2^- \longrightarrow 2H_2O + 2NO + I_2$$

For NO release experiments, samples were placed in a thermostated quartz cell (1 cm path length, 3 mL capacity) and irradiated at λ 405 nm under gentle stirring careful was taken to avoid the laser illumination of the electrode within the cell, which may result in false NO signals due to photoelectric artifacts.

2.4. Isothermal Titration Calorimetry (ITC) measurements

Canavalia ensiformis (Jack bean) concanavalin A (ConA) lectin (type VI, lyophilised powder) was purchased from Sigma and used as received. All solutions were prepared in MilliQ pure water (18.2 MΩcm) and degassed for 10 min and thermostated prior each experiment. UV-Vis spectroscopy was used to calculate the lectin solution concentration ($A^{1\%}_{280\ nm}$ = 13.7 for the tetrameric form). ITC experiments were performed on an ultrasensitive VP-ITC (Microcal Inc., Northampton, MA) as as previously described elsewhere (Casas-Solvas, Ortiz-Salmerón, García-Fuentes, & Vargas-Berenguel, 2008) and the calculus were performed using Origin software (provided by the instrument). Briefly, the calorimeter was calibrated as recommended by the manufacturer. The reference and sample cells were filled with degassed MilliQ water and the protein solution, respectively. The sample cell was continuously stirred at 320 rpm. Solutions of the mannosylated βCDs and ConA (see table S1 at supporting information for concentrations) were prepared in 20 mM phosphate buffer (pH 7.2) containing 20 mM NaCl, 100 µM $CaCl_2$ and 100 µM $MnCl_2$. Each mannosylated βCD was injected in 8-10 µL portions every 5 min with a 250 µL syringe. The mannosylated βCDs were also injected into pure buffer in separate experiments in order to obtain the corresponding dilution background profiles, which turned out to be similar to the residual heat signals detected after saturation in the interaction experiments with the protein. Obtained thermograms depicted the transfer of heat per second following each injection of mannosylated βCD into the ConA solution as a function of time. The integration of each peak gave the amount of heat generated by each injection after subtracting the mannosylated βCD dilution heat. The best fit of the experimental data to the model of equal and independent sites provided the binding constant and the thermodynamic profile along with the corresponding standard deviations.

For these calculations, $\Delta H = \Delta H^0$ was assumed and the changes in the standard free energy ΔG^0 and entropy ΔS^0 were determined as $\Delta G^0 = -RT\ln K$ and $T\Delta S^0 = \Delta H - \Delta G^0$.

*2.5. Synthesis of propargyl 6-O-benzoyl-α-D-mannopyranoside **4***

A solution of BzCN (210 µL, 232 mg, 1.77 mmol) in dry DMF (2 mL) and catalytic amount of dry Et_3N (20 µL, 14 mg, 0.0.138 mmol) were added dropwise to a solution of propargyl α-D-mannopyranoside **3** (300 mg, 1.375 mmol) in dry DMF (10 mL) at -40 °C (CH_3CN/dry ice bath). After 3 hours at that temperature, the reaction was quenched by adding 4 mL of MeOH and left warming up to room temperature. The solvent was rotary evaporated and the crude product was purified by column chromatography using CH_2Cl_2-MeOH (50:1→25:2) as eluent to yield propargyl 6-*O*-benzoyl-α-D-mannopyranoside **4** (204 mg, 0.633 mmol, 46%) as a colorless oil. R_f = 0.29 (CH_2Cl_2-MeOH 25:2); $[\alpha]_D$ +60.8º (*c* 1, CH_2Cl_2); IR ν/cm^{-1} 3296, 2934, 1715, 1266, 1049, 712; ^{1}H-NMR (300 MHz, $CDCl_3$) δ (ppm) 7.99 (app dt, 2H, J_{app} = 6.9 Hz, J_{app} = 1.5 Hz, H_{Bz}-2'), 7.50 (app tt, 1H, J_{app} = 7.3 Hz, J_{app} = 1.6 Hz, H_{Bz}-4'), 7.38 (app tt, 2H, J_{app} = 7.3 Hz, J_{app} = 1.6 Hz, H_{Bz}-3'), 4.99 (d, 1H, $^3J_{1,2}$ = 1.3 Hz, H-1), 4.59 (app bd, 2H, J_{app} = 3.0 Hz, H-6$^{(a,b)}$), 4.22 (dd, 1H, $^2J_{CHO,CHO}$ = 15.7 Hz, $^4J_{CHO,\equiv CH}$ = 2.5 Hz, CHO), 4.15 (dd, 1H, $^2J_{CHO,CHO}$ = 15.7 Hz, $^4J_{CHO,\equiv CH}$ = 2.5 Hz, CHO), 4.02-3.93 (bs, 4H, H-2, OH), 3.88-3.85 (m, 3H, H-3,4,5), 2.41 (t, 1H, $^4J_{CHO,\equiv CH}$ = 2.5 Hz, ≡CH); ^{13}C-RMN (75 MHz, $CDCl_3$) δ (ppm) 167.3 (CO), 133.3 (CH_{Bz}-4'), 129.9 (CH_{Bz}-2'), 129.8 (C_{Bz}-1'), 128.5 (CH_{Bz}-3'), 98.7 (C-1), 78.8 (*C*≡CH), 75.2 (C≡*C*H), 71.5 (C-3 or C-5), 71.3 (C-3 or C-5), 70.6 (C-2), 67.8 (C-4), 64.6 (C-6), 54.5 (CH_2O); MALDI-TOF-MS *m/z* calcd for $C_{16}H_{18}O_7Na^+$ 345.1, found 345.0 $(M + Na)^+$; *m/z* calcd for $C_{16}H_{18}O_7K^+$ 361.2, found 361.0 $(M + K)^+$.

*2.6. Synthesis of propargyl 2-O-acetyl-6-O-benzoyl-α-D-mannopyranoside **5***

Trimethyl orthoacetate (472 µL, 445 mg, 3.7 mmol) was added at once to a solution of propargyl 6-*O*-benzoyl-α-D-mannopyranoside **4** (398 mg, 1.23 mmol) and camphorsulfonic acid (57 mg, 0.246 mmol) in dry CH_3CN (12 mL) at room temperature. After 1.5 hours the reaction was quenched with Et_3N (165 µL). The solvent was rotary evaporated at 40 °C and the colorless oily residue was dissolved in EtOAc (40 mL) and washed with 1M HCl (40 mL). The organic phase was dried over anhydrous $MgSO_4$ and solvent was rotary evaporated. The crude product was purified by column chromatography using CH_2Cl_2-MeOH (50:1→25:1) as eluent to yield propargyl 2-*O*-acetyl-6-*O*-benzoyl-α-D-mannopyranoside **5** (408 mg, 1.12 mmol, 91%) as a colorless oil. R_f = 0.26 (CH_2Cl_2-MeOH 25:1); Mp: 113 ºC; $[\alpha]_D$ +43.5º (*c* 1, CH_2Cl_2); IR ν/cm^{-1} 3445, 2936, 1718, 1266, 1067, 713; ^{1}H-NMR (300 MHz, $CDCl_3$) δ (ppm) 8.07 (app dt, 2H, J_{app} = 6.9 Hz, J_{app} = 1.4 Hz, H_{Bz}-2'), 7.57 (app tt, 1H, J_{app} = 7.4 Hz, J_{app} = 1.6 Hz, H_{Bz}-4'), 7.44 (app tt, 2H, J_{app} = 7.4 Hz, J_{app} = 1.4 Hz, H_{Bz}-3'), 5.18 (dd, 1H, $^3J_{2,3}$ = 3.5 Hz, $^3J_{1,2}$ = 1.6 Hz, H-2), 5.02 (d, 1H, $^3J_{1,2}$ = 1.6 Hz, H-1), 4.71 (dd, 1H, $^2J_{6a,6b}$ = 12.2 Hz, $^3J_{5,6a}$ = 4.6 Hz, H-6a), 4.55 (dd, 1H, $^2J_{6a,6b}$= 12.2 Hz; $^3J_{5,6b}$ = 2.1 Hz, H-6b), 4.28 (dd, 1H, $^2J_{CHO,CHO}$ = 15.8 Hz, $^4J_{CHO,\equiv CH}$ = 2.4 Hz, CHO), 4.23 (dd, 1H, $^2J_{CHO,CHO}$ = 15.8 Hz, $^4J_{CHO,\equiv CH}$ = 2.4 Hz, CHO), 4.08 (dd, 1H, $^3J_{3,4}$ = 9.4 Hz; $^3J_{2,3}$ = 3.5 Hz, H-3), 3.91 (ddd, $^3J_{4,5}$ = 6.6 Hz, $^3J_{5,6a}$ = 4.6 Hz, $^3J_{5,6b}$ = 2.1 Hz, H-5), 3.79 (app t, 1H, J_{app} = 9.7 Hz, H-4), 2.45 (t, 1H, $^4J_{CHO,\equiv CH}$ = 2.4 Hz, ≡CH), 2.08 (s, 3H, CH_3); ^{13}C-RMN (75 MHz, $CDCl_3$) δ (ppm) 170.9 (CO), 167.2 (CO_{Bz}), 133.5 (CH_{Bz}-4'), 129.9 (CH_{Bz}-2'),129.8 (C_{Bz}-1'), 128.6 (CH_{Bz}-3'), 96.6 (C-1), 78.4 (*C*≡CH), 75.4 (C≡*C*H) 71.8 (C-2), 71.3 (C-5), 69.8 (C-4), 67.8 (C-3), 63.9 (C-6), 54.9 (CH_2O), 21.0 (CH_3). MALDI-TOF-MS *m/z* calcd for $C_{18}H_{20}O_8Na^+$ 387.12, found 387.0 $(M + Na)^+$; *m/z* calcd for $C_{18}H_{20}O_8K^+$ 403.1, found 403.0 $(M + K)^+$.

*2.7. Synthesis of propargyl 2-O-acetyl-3,4,6-tri-O-benzoyl-α-D-mannopyranoside **6***

Bz_2O (609 mg, 2.69 mmol), catalytic amount of Et_3N (375 µL, 272 mg, 2.69 mmol) and 4-dimethylaminopyridine (4-DMAP) (2 mg, 0.015 mmol) were subsequently added to a solution of propargyl 2-*O*-acetyl-6-*O*-benzoyl-α-D-mannopyranoside **5** (327 mg, 0.897 mmol) in dry CH_2Cl_2 (17 mL). After 1.5 hours solvent was rotary evaporated and the colorless oily residue was dissolved in EtOAc (45 mL) and washed with 1M HCl (45 mL), saturated aq. $NaHCO_3$ (45 mL), and H_2O (45 mL). The organic phase was dried over anhydrous $MgSO_4$ and solvent was rotary evaporated. The crude product was purified by column chromatography using hexane-EtOAc (2:1) as eluent to yield propargyl 2-*O*-acetyl-3,4,6-tri-*O*-benzoyl-α-D-mannopyranoside **6** (491 mg, 0.858 mmol, 95%) as a colorless oil. R_f = 0.63 (hexane-EtOAc 2:1); $[\alpha]_D$ +36.5º (*c* 0.5, CH_2Cl_2); IR ν/cm^{-1} 2958, 1725, 1267, 1108, 710. ^{1}H-NMR (300 MHz, $CDCl_3$) δ (ppm) 8.05 (app dt, 2H, J_{app} = 6.9 Hz, J_{app} = 1.5 Hz, H_{Bz}-2'), 7.95 (app dt, 2H, J_{app} = 6.9 Hz, J_{app} = 1.5 Hz, H_{Bz}-2'), 7.89 (app dt, 2H, J_{app} = 6.9 Hz, J_{app} = 1.5 Hz, H_{Bz}-2'), 7.58-7.46 (m, 3H, H_{Bz}-4'), 7.44-7.32 (m, 6H, H_{Bz}-3'), 5.94 (app t, 1H, J_{app} = 10.0 Hz, H-4), 5.80 (dd, 1H, $^3J_{3,4}$ = 10.0 Hz, $^3J_{2,3}$ = 3.3 Hz, H-3), 5.51 (dd, 1H, $^3J_{2,3}$ = 3.3 Hz, $^3J_{1,2}$ = 1.8 Hz, H-2), 5.17 (d, 1H, $^3J_{1,2}$ = 1.8 Hz, H-1), 4.63 (dd, 1H, $J_{6a,6b}$ = 11.9 Hz, $J_{5,6}$ = 2.9 Hz, H-6a), 4.48 (dd, 1H, $J_{6a,6b}$ = 11.9 Hz, $J_{5,6b}$ = 5.1 Hz, H-6b), 4.44-4.39 (m, 1H, H-5), 4.38 (app d, 2H, J_{app} = 2.4 Hz, CH_2O), 2.49 (t, 1H, $^4J_{CHO,\equiv CH}$ = 2.4Hz, ≡CH), 2.15 (s, 3H, CH_3). ^{13}C-RMN (75 MHz, $CDCl_3$) δ (ppm) 169.9 (CO), 166.3 (CO_{Bz}), 165.7 (CO_{Bz}), 165.6 (CO_{Bz}), 133.8-133.3 (CH_{Bz}-4'), 130.3-129.1 (C_{Bz}-1'. CH_{Bz}-2'), 128.6-128.5 (CH_{Bz}-3'), 96.4 (C-1), 78.2 (C≡), 75.2 (≡CH), 69.9 (C-2 or C-3), 69.8 (C-2 or C-3), 69.5 (C-5), 67.1 (C-4), 63.3 (C-6), 55.3 (CH_2O), 20.9 (CH_3). MALDI-TOF-MS *m/z* calcd for $C_{32}H_{28}O_{10}$ 572.17, found 572.9 $(M)^+$.

*2.8. Synthesis of propargyl 3,4,6-tri-O-benzoyl-α-D-mannopyranoside **7***

A 7% HCl in MeOH stock solution (3.14 mL) was added to a solution of propargyl 2-*O*-acetyl-3,4,6-tri-*O*-benzoyl-α-D-mannopyranoside **6** (85 mg, 0.148 mmol) in dry CH_3CN (2 mL) and stirred for 3 days at room temperature until the disappearance of the starting material. Solvent was rotary evaporated and the light green oily residue was dissolved in EtOAc (10 mL), washed with saturated aq. $NaHCO_3$ (2x25 mL) and H_2O (25 mL). The organic phase was dried over anhydrous $MgSO_4$ and solvent was rotary evaporated. The crude product was purified by column chromatography using hexane-EtOAc (3:1→5:2) as eluent to yield propargyl 3,4,6-tri-*O*-benzoyl-α-D-mannopyranoside **7** (64.5 mg, 0.122 mmol, 82%) as a colorless oil. R_f = 0.44 (hexane-EtOAc 2:1); $[\alpha]_D$ +48.0º (*c* 1, CH_2Cl_2); IR ν/cm^{-1} 2955, 1723, 1452, 1266, 710. ^{1}H-NMR (300 MHz, $CDCl_3$) δ (ppm) 8.02 (app dt, 2H, J_{app} = 6.9 Hz, J_{app} = 1.5 Hz, H_{Bz}-2'), 7.98-7.92 (m, 4H, H_{Bz}-2'), 7.56-7.45 (m, 3H, H_{Bz}-4'), 7.42-7.30 (m, 6H, H_{Bz}-3'), 5.97 (app t, 1H, J_{app} = 10.0 Hz, H-4), 5.68 (dd, 1H, $^3J_{3,4}$ = 10.0 Hz, $^3J_{2,3}$ = 3.2 Hz, H-3), 5.21 (d, 1H, $^3J_{1,2}$ = 1.7 Hz, H-1), 4.59 (dd, 1H, $^2J_{6a,6b}$ = 12.0 Hz, $^3J_{5,6}$ = 3.1 Hz, H-6a), 4.49 (dd, 1H, $^2J_{6a,6b}$ = 12.0 Hz, $J_{5,6}$ = 5.2 Hz, H-6b), 4.40 (dd, 1H, $^3J_{2,3}$ = 3.2 Hz, $^3J_{1,2}$ = 1.7 Hz, H-2), 4.38 (app d, 2H, J_{app} = 2.4 Hz, CH_2O), 4.36-4.34 (m, 1H, H-5), 2.49 (t, 1H, $^4J_{CHO,\equiv CH}$ = 2.4 Hz, ≡CH); ^{13}C-RMN (75 MHz, $CDCl_3$) δ (ppm) 166.4-165.6 (CO_{Bz}), 133.5-133.2 (CH_{Bz}-4'), 130.1-129.2 (C_{Bz}-1', CH_{Bz}-2'), 128.7-128.6 (CH_{Bz}-3'), 98.4 (C-1), 78.9 (C≡), 75.5 (≡CH), 72.6 (C-2), 69.4 (C-3 or C-5), 69.3 (C-3 or C-5), 67.0 (C-4), 63.5 (C-6), 55.1 (CH_2O). MALDI-TOF-MS *m/z* calcd for $C_{30}H_{26}O_9Na^+$ 553.16, found 553.1 $(M+Na)^+$.

*2.9. Synthesis of propargyl O-(2,3,4,6-tetra-O-benzoyl-α-D-mannopyranosyl)-(1→2)-3,4,6-tri-O-benzoyl-α-D-mannopyranoside **9***

A mixture of propargyl 3,4,6-tri-*O*-benzoyl-α-D-mannopyranoside **7** (140 mg, 0.264 mmol) and 2,3,4,6-tetra-*O*-benzoyl-α-D-mannopyranosyl trichloroacetimidate **8** (240 mg, 0.325 mmol) was

co-evaporated three times from toluene and the white residue dried under vacuum in the presence of 4 Å molecular sieves for 1.5 h. The mixture was dissolved in dry CH_2Cl_2 (9.5 mL) and stirred at 0 °C for 15 min. A catalytic amount of TMSOTf (9.6 µL, 0.0528 mmol) was added and stirred at 0 °C for 2 h. Et_3N (100 µL) was added, and the mixture was filtered over a pad of Celite (1.5 cm). Solvent was rotary evaporated and the crude product was purified by column chromatography using CH_2Cl_2-MeOH (500:1→200:1) to yield propargyl *O*-(2,3,4,6-tetra-*O*-benzoyl-α-D-mannopyranosyl)-(1→2)-3,4,6-tri-*O*-benzoyl-α-D-mannopyranoside **9** (150 mg, 0.135 mmol, 51%) as a white foamy solid. R_f = 0.54 (hexane-EtOAc 2:1); Mp 121 ºC; $[\alpha]_D$ -28.5º (*c* 1, CH_2Cl_2); IR ν/cm^{-1} 2957, 1724, 1264, 1107, 708. ^{1}H-NMR (600 MHz, $CDCl_3$) δ (ppm) 8.10-8.08 (m, 4H, H_{Bz}-2'), 8.03 (app dd, 2H, J_{app} = 8.4 Hz, J_{app} = 1.2 Hz, H_{Bz}-2'), 7.98 (app dd, 2H, J_{app} = 8.4 Hz, J_{app} = 1.2 Hz, H_{Bz}-2'), 7.95 (app dd, 2H, J_{app} = 8.4 Hz, J_{app} = 1.2 Hz, H_{Bz}-2'), 7.93 (app dd, 2H, J_{app} = 8.4 Hz, J_{app} = 1.2 Hz, H_{Bz}-2'), 7.87 (app dd, 2H, J_{app} = 8.4 Hz, J_{app} = 1.2 Hz, H_{Bz}-2'), 7.60-7.43 (m, 7H, H_{Bz}-4'), 7.42-7.28 (m, 14H, H_{Bz}-3'), 6.12 (app t, 1H, J_{app} = 10.1 Hz, H-4^B), 6.04 (app t, 1H, J_{app} = 9.9 Hz, H-4^A), 6.02 (dd, 1H, $^3J_{3B,4B}$ = 10.1 Hz, $^3J_{2B,3B}$ = 3.3 Hz, H-3^B), 5.91 (dd, 1H, $^3J_{2B,3B}$ = 3.3 Hz, $^3J_{1B,2B}$ = 1.7 Hz, H-2^B), 5.90 (dd, 1H, $^3J_{2A,3A}$ = 3.1 Hz, $^3J_{3A,4A}$ = 9.9 Hz, H-3^A), 5.41 (d, 1H, $^3J_{1A,2A}$ = 2.0 Hz, H-1^A), 5.28 (d, 1H, $^3J_{1B,2B}$ = 1.7 Hz, H-1^B), 4.71 (dd, 1H, $^2J_{6B(a,b)}$ = 12.2 Hz, $^3J_{5B,6Ba}$ = 2.7 Hz, H-6^{Ba}), 4.65 (dd, 1H, $^2J_{6A(a,b)}$ = 12.2 Hz, $^3J_{5A,6Aa}$ = 3.0 Hz, H-6^{Aa}), 4.61 (ddd, 1H, $^3J_{4B,5B}$ = 10.0 Hz, $^3J_{5B,6Bb}$ = 4.4 Hz, $^3J_{5B,6Ba}$ = 2.7 Hz, H-5^B), 4.57 (dd, 1H, $^2J_{6A(a,b)}$ = 12.2 Hz, $^3J_{5A,6Ab}$ = 5.3 Hz, H-6^{Ab}), 4.47 (dd, 1H, $^2J_{6B(a,b)}$ = 12.2 Hz, $^3J_{5B,6Bb}$ = 4.4 Hz, H-6^{Bb}), 4.43 (ddd, 1H, $^3J_{4A,5A}$ = 10.0 Hz, $^3J_{5A,6Ab}$ = 5.3 Hz, $^3J_{5A,6Aa}$ = 3.0 Hz, H-5^A), 4.41 (dd, 1H, $^3J_{2A,3A}$ = 3.1 Hz, $^3J_{1A,2A}$ = 2.0 Hz, H-2^A), 4.34 (dd, 1H, $^2J_{CHO,CHO}$ = 15.8 Hz, $^4J_{CHO,\equiv CH}$ = 2.4 Hz, CHO), 4.29 (dd, 1H, $^2J_{CHO,CHO}$ = 15.8 Hz, $^4J_{CHO,\equiv CH}$ = 2.4 Hz, CHO), 2.52 (t, 1H, $^4J_{CHO,\equiv C}$ = 2.4 Hz, ≡CH); ^{13}C-RMN (150 MHz, $CDCl_3$) δ (ppm) 166.5-165.0 (CO), 133.6-133.2 (CH_{Bz}-4'), 130.2-129.8 (CH_{Bz}-2'), 129.3-129.0 (C_{Bz}-1'), 128.7-128.5 (CH_{Bz}-3'), 99.8 (C-1^B), 97.5 (C-1^A), 78.3 (C≡), 76.9 (C-2^A overlapped with $CDCl_3$ signal), 75.9 (≡CH), 70.6 (C-3^A), 70.2 (C-2^B), 69.9 (C-5^B), 69.8 (C-3^B), 69.6 (C-5^A), 67.7 (C-4^A), 66.9 (C-4^B), 63.7 (C-6^A), 62.9 (C-6^B), 55.3 (CH_2O). MALDI-TOF-MS *m/z* calcd for $C_{64}H_{52}O_{18}Na^+$ 1131.3, found 1131.1 $(M+Na)^+$; calcd for $C_{64}H_{52}O_{18}K^+$ 1147.3, found 1147.1 $(M+K)^+$

*2.10. Synthesis of propargyl α-D-mannopyranosyl-(1→2)-α-D-mannopyranoside **10***

Propargyl *O*-(2,3,4,6-tetra-*O*-benzoyl-α-D-mannopyranosyl)-(1→2)-3,4,6-tri-*O*-benzoyl-α-D-mannopyranoside **9** (3.14 g, 0.0028 mol) was sonicated in dry MeOH (188 mL) until a clear solution was formed. Then, NaOMe in dry MeOH was added until pH 12 and the mixture was stirred for 4 hours. The pH was neutralized with 0.1N HCl and solvent was rotary evaporated. The crude product was purified by column chromatography using EtOAc-MeOH (3:2) as eluent to give propargyl α-D-mannopyranosyl)-(1→2)-α-D-mannopyranoside **10** (1 g, 94%) as an hygroscopic white powder after lyophilization. R_f = 0.54 (EtOAc-MeOH 1:1); $[\alpha]_D$ +49.3º (*c* 1, H_2O); IR ν/cm^{-1} 3332, 2945, 1727, 1449, 1022. ^{1}H-RMN (600 MHz, D_2O) δ (ppm) 5.27 (d, 1H, $^3J_{1A,2A}$ = 1.7 Hz, H-1^A), 5.02 (d, 1H, $^3J_{1B,2B}$ = 1.8 Hz, H-1^B), 4.36 (dd, 1H, $^2J_{CHO,CHO}$ = 16.0 Hz, $^4J_{CHO,\equiv CH}$ = 2.4 Hz, CHO), 4.29 (dd, 1H, $^2J_{CHO,CHO}$ = 16.0 Hz, $^4J_{CHO,\equiv CH}$ = 2.4 Hz, CHO), 4.08 (dd, 1H, $^3J_{2B,3B}$ = 3.3 Hz, $^3J_{1B,2B}$ = 1.8 Hz, H-2^B), 3.97 (dd, 1H, $^3J_{2A,3A}$ = 3.4 Hz, $^3J_{1A,2A}$ = 1.7 Hz, H-2^A), 3.94-3.81 (m, 4H, H-3^{A,B}, 6$^{A(a,b)}$), 3.80-3.69 (m, 4H, H-4^A, 5^B, 6$^{B(a,b)}$), 3.66-3.58 (m, 2H, H-4^B, 5^A), 2.91 (t, 1H, $^4J_{CHO,\equiv CH}$ = 2.4 Hz, ≡CH); ^{13}C-RMN (150 MHz, D_2O) δ (ppm) 102.4 (C-1^B), 97.0 (C-1^A), 78.8 (C≡), 78.7 (C-2^A), 76.2 (≡CH), 73.2 (C-5^A), 73.1 (C-5^B), 70.3 (C-3^B), 70.0 (C-2^B), 69.9 (C-3^A), 66.8 (C-4^B), 66.7

(C-4^{A}), 61.0 (C-6^{A}), 60.7 (C-6^{B}), 54.5 (CH_2O). ESI$^+$ *m/z* calcd for $C_{15}H_{24}O_{11}Na^+$ 403.13 found 403.51.

2.11. Synthesis of 6^{I}-deoxy-6^{I}-[4-(α-D-mannopyranosyloxymethyl)-1H-1,2,3-triazol-1-yl]-6^{X}-deoxy-6^{X}-N-{3'-[N'-(4''-nitro-3''-trifluoromethylphen-1''-yl)amino]propylamino}cyclomaltoheptaose ***ManNOPDβCD***

A suspension of CuI (9.5 mg, 0.05 mmol) in H_2O (15 mL) was added to a pre-heated (90 °C) solution of propargyl α-D-mannoside **3** (46.6 mg, 0.213 mmol) and 6^{I}-deoxy-6^{I}-azido-6^{X}-deoxy-6^{X}-*N*-{3-[*N'*-(4'-nitro-3'-trifluoromethylphen-1'-yl)amino]propylamino}cyclomaltoheptaose **1** (200 mg, 0.142 mmol) in DMF (15 mL). The mixture was stirred for 2 h at 100 °C and overnight at rt. Solvents were evaporated under high vacuum and the crude product was purified by column chromatography using CH_3CN-H_2O-(30% v/v aq. NH_3) (20:5:2→10:5:1) as eluent. The obtained material was dialyzed to yield **ManNOPDβCD** (160 mg, 0.099 mmol, 71 %) as a light-sensitive yellow solid. R_f = 0.42 (CH_3CN-H_2O-(30% v/v aq. NH_3) 10:5:1); IR (KBr) ν/cm^{-1} 3386, 2929, 1612, 1330, 1156, 1031. ^{1}H-NMR (600 MHz,$CDCl_3$) δ (ppm) 8.31-8.22 (m, H^{ar}), 8.15-8.11 (m, H^{ar}), 8.06 (s, H-5-C_2HN_3), 6.95-6.90 (m, H^{ar}), 6.82-6.73 (bs, NH), 5.38-4.53 (m, H-1^{I,X,CD,A},6$^{I(a,b)}$, CH_2O, overlapped with HDO), 4.29-3.16 (m, H-2^{I,X,CD,A},3^{I,X,CD,A},4^{I,X,CD,A},5^{I,X,CD,A},6$^{CD(a,b),A(a,b)}$, C*H*$_2$NHPh), 3.11-2.45 (m, H-6$^{X(a,b)}$, C*H*$_2$NH), 1.86-1.70 (m, CH_2). ^{13}C-NMR (150 MHz, $CDCl_3$) δ (ppm) 152.4 (C^{ar}), 143.5-143.4 (C-4-C_2HN_3), 134.9 (C^{ar}), 130.0 (C^{ar}), 127.3-126.5 (C-5-C_2HN_3, C^{ar}), 122.3 (q, $^1J_{C,F}$ = 270.9 Hz, CF_3), 111.3 (C^{ar}), 102.8-101.5 (C-1^{I,X,CD}), 99.9-99.4 (C-1^{CD,A}), 94.0-93.7 (C-1^{CD}), 84.0-80.9 (C-4^{I,X,CD}), 73.1-70.0 (C-2^{I,X,CD,A},3^{I,X,CD,A},5^{I,X,CD,A}), 66.8-66.7 (C-4^{A}), 60.9-58.6 (C-6^{CD,A}, CH_2O), 51.3-50.7 (C-6^{I,X}), 44.8 (*C*H$_2$NH), 40.6 (*C*H$_2$NHPh), 26.0 (CH_2). ESI$^+$ *m/z* calcd for $C_{61}H_{94}F_3N_6O_{41}^+$ 1624.4 found 1624.5 $(M+H)^+$.

2.12. Synthesis of 6^{I}-deoxy-6^{I}-[4-(α-D-mannopyranosyl-(1→2)-α-D-mannopyranosiloxymethyl)-1H-1,2,3-triazol-1-yl]-6^{X}-deoxy-6^{X}-N-{3'-[N'-(4''-nitro-3''-trifluoromethylphen-1''-yl)amino]propylamino}cyclomaltoheptaose ***BiManNOPDβCD***

A suspension of CuI (5.9 mg, 0.031 mmol) in H_2O (9.2 mL) was added to a pre-heated solution (90 °C) of propargyl α-D-mannopyranosyl)-(1→2)-α-D-mannopyranoside **10** (50 mg, 0.131 mmol) and 6^{I}-deoxy-6^{I}-azido-6^{X}-deoxy-6^{X}-*N*-{3-[*N'*-(4'-nitro-3'-trifluoromethylphen-1'-yl)amino]propylamino}cyclomaltoheptaose **1** (123 mg, 0.088 mmol) in DMF (9.2 mL). The mixture was stirred for 2 hours at 100 °C and overnight at rt. Solvents were evaporated under high vacuum and the crude product was purified by column chromatography using CH_3CN-H_2O-(30% v/v aq. NH_3) (10:5:1→20:15:2) as eluent. The obtained material was dialyzed to yield **BiManNOPDβCD** (49 mg, 0.027 mmol, 88%) as a light-sensitive yellow solid. R_f = 0.29 (CH_3CN-H_2O-(30% v/v aq. NH_3) 10:5:1); IR (KBr) ν/cm^{-1} 3416, 2927, 1612, 1329, 1155, 1032. ^{1}H-NMR (600 MHz, $CDCl_3$) δ (ppm) 8.32-8.22 (m, H^{ar}), 8.16-8.11 (m, H^{ar}), 8.06 (s, H-5-C_2HN_3), 6.97-6.90 (m, H^{ar}), 6.83-6.78 (bs, NH), 5.40-4.53 (m, H-1^{I,X,CD,A,B},6$^{I(a,b)}$, CH_2O, overlapped with HDO), 4.26-3.17 (m, H-2^{I,X,CD,A,B},3^{I,X,CD,A,B},4^{I,X,CD,A,B},5^{I,X,CD,A,B},6$^{X(a,b),CD(a,b),A(a,b),B(a,b)}$, C*H*$_2$NHPh), 3.11-2.45 (m, H-6$^{X(a,b)}$, C*H*$_2$NH), 1.86-1.70 (m, CH_2). ^{13}C-NMR (150 MHz, $CDCl_3$) δ (ppm) 153.8-153.1 (C^{ar}), 144.2-143.9 (C-4-C_2HN_3), 135.5 (C^{ar}), 130.7 (C^{ar}), 127.9-127.0 (C-5-C_2-HN_3, C^{ar}), 123.5 (q, $^1J_{C,F}$ = 273.4 Hz, CF_3), 111.9 (C^{ar}), 103.4-102.0 (C-1^{I,X,CD,B}), 99.1-98.6 (C-1^{CD,A}), 93.2 (C-1^{CD}), 84.7-79.2 (C-2^{A},4^{I,X,CD}), 73.9-70.6 (C-2^{I,X,CD,A,B},3^{I,X,CD,A,B},5^{I,X,CD,A,B}), 67.7-67.5 (C-4^{A,B}), 61.7-59.3 (C-6^{CD,A,B}, CH_2O), 52.0-51.9 (C-6^{I,X}), 47.9-45.4 (CH_2NH), 41.7-41.1 (CH_2NHPh), 26.3 (CH_2). ESI$^+$ *m/z* calcd for $C_{67}H_{104}F_3N_6O_{46}^+$ 1786.6 found 1786.6 $(M+H)^+$.

*2.13. Synthesis of 6^{I}-deoxy-6^{I}-[4-(α-D-mannopyranosyloxymethyl)-1H-1,2,3-triazol-1-yl]cyclomaltoheptaose **ManβCD***

Compound **ManβCD** was prepared by modifying a previously reported method (Gade et al., 2016). CuI (0.057 g, 0.302 mmol) was added to a preheated (100 ºC) solution of 6^{I}-azide-6^{I}-deoxycyclomaltoheptaose **2** (1 g, 0.862 mmol) and propargyl α-D-mannoside **3** (0.282 g, 1.292 mmol) in a mixture of DMF (75 mL) and water (75 mL). After 16 hours at that temperature, the solvent was rotary evaporated and the crude product was purified by column chromatography using CH_3CN-H_2O-(30% v/v aq. NH_3) 20:15:2 as eluent to yield 6^{I}-deoxy-6^{I}-[4-(α-D-mannopyranosyloxymethyl)-1*H*-1,2,3-triazol-1-yl]cyclomaltoheptaose **ManβCD** (1.093 g, 0.793 mmol, 92 %) as a white solid. R_f = 0.41 (CH_3CN-H_2O-(30% v/v aq. NH_3) 20:15:2); Mp 233 ºC (dec); $[\alpha]_D$ +114.2º (*c* 1, H_2O); IR (KBr) ν/cm^{-1} 3387, 2928, 1641, 1412, 1156, 1029, 581; ^{1}H-RMN (600 MHz, D_2O) δ (ppm) 8.14 (s, 1H, H-5-C_2HN_3), 5.20 (d, 1H, $^3J_{1,2}$ = 3.8 Hz, H-1^{VII}), 5.10-5.08 (m, 4H, H-1^{III-VI}), 5.05 (bd, 1H, $^2J_{6a,6b}$ = 14.6 Hz, H-6^{Ia}), 5.03 (d, 1H, $^3J_{1,2}$ = 3.8 Hz, H-1^{II}), 5.02 (d, 1H, $^3J_{1,2}$ = 1.6 Hz, H-1^{A}), 5.01 (d, 1H, $^3J_{1,2}$ = 3.6 Hz, H-1^{I}), 4.86 (bd, 1H, ^2J = 12.1 Hz, CH^{a}O), 4.69 (bd, 1H, ^2J = 12.1 Hz, CH^{b}O), 4.65 (dd, 1H, $^2J_{6a,6b}$ = 14.6 Hz, $^3J_{5,6b}$ = 9.4 Hz, H-6^{Ib}), 4.25 (t, 1H, *J* = 9.5 Hz, H-5^{I}), 4.03 (t, 1H, *J* = 9.6 Hz, H-3^{VII}), 4.02-3.96 (m, 8H, H-2^{A},3$^{I,III-VI}$,5^{VII}), 3.95-3.85 (m, 17H, H-3^{II},5$^{III-VII}$,6$^{(III-VII)(a,b)}$,6^{Aa}), 3.81-3.79 (m, 3H, H-3^{A},5^{A},6^{Ab}), 3.72 (dd, 1H, $^3J_{2,3}$ = 10.1 Hz, $^3J_{1,2}$ = 3.8 Hz, H-2^{VII}), 3.70-3.66 (m, 6H, H-2$^{I,III-VI}$,4^{A}), 3.65-3.59 (m, 6H, H-2^{II},4$^{III-VII}$), 3.58-3.53 (m, 3H, H-4^{I,II},5^{II}), 3.18 (bd, 1H, $^2J_{6a,6b}$ = 12.3 Hz, H-6^{IIa}), 2.83 (bd, 1H, $^2J_{6a,6b}$ = 12.3 Hz, H-6^{IIb}); ^{13}C-RMN (150 MHz, D_2O) δ (ppm) 143.4 (C-4-C_2HN_3), 126.8 (C-5-C_2HN_3), 102.0 (C-1^{VII}), 101.9-101.8 (C-1^{II-VI}), 101.4 (C-1^{I}), 99.5 (C-1^{A}), 83.1 (C-4^{I}), 81.2-80.6 (C-4^{II-VII}), 73.0-71.5 (C2^{I-VII},3^{I-VII},5$^{II-VII,A}$), 70.5 (C-3^{A}), 70.4 (C-5^{I}), 70.0 (C-2^{A}), 66.6 (C-4^{A}), 60.9 (C-6^{A}), 60.3-60.2 (C-6$^{III-VII}$), 59.6 (CH_2O), 59.2 (C-6^{II}), 51.2 (C-6^{I}); MALDI-TOF-MS *m*/*z* calcd for $C_{51}H_{83}N_3O_{40}Na^+$ 1400.4, found 1400.2 $(M + Na)^+$.

*2.14. Synthesis of 6^{I}-deoxy-6^{I}-[4-(α-D-mannopyranosyl-(1→2)-α-D-mannopyranosyloxymethyl)-1H-1,2,3-triazol-1-yl]cyclomaltoheptaose **BiManβCD***

CuI (0.006 g, 0.030 mmol) was added to a preheated (100 ºC) solution of 6^{I}-azide-6^{I}-deoxycyclomaltoheptaose **2** (0.100 g, 0.086 mmol) and propargyl α-D-mannopyranosyl-(1→2)-α-D-mannopyranoside **10** (0.050 g, 0.131 mmol) in a mixture of DMF (7.5 mL) and water (7.5 mL). After 16 hours at that temperature, the solvent was rotary evaporated and the crude product was purified by column chromatography using CH_3CN-H_2O-(30% v/v aq. NH_3) 20:15:2 as eluent to yield 6^{I}-deoxy-6^{I}-[4-(α-D-mannopyranosyl-(1→2)-α-D-mannopyranosyloxymethyl)-1*H*-1,2,3-triazol-1-yl]cyclomaltoheptaose **BiManβCD** (0.119 g, 0.077 mol, 90 %) as a white solid. R_f = 0.24 (CH_3CN-H_2O-(30% v/v aq. NH_3) 20:15:2); Mp 219 ºC (dec); $[\alpha]_D$ +106.1º (*c* 1, H_2O); IR (KBr) ν/cm^{-1} 3386, 2929, 1658, 1412, 1155, 1079, 1031, 472; ^{1}H-RMN (500 MHz, D_2O) δ (ppm) 8.09 (s, 1H, H-5-C_2HN_3), 5.21 (d, 1H, $^3J_{1,2}$ = 1.5 Hz, H-1^{A}), 5.17 (d, 1H, $^3J_{1,2}$ = 3.8 Hz, H-1^{VII}), 5.07-5.05 (m, 4H, H-1^{III-VI}), 5.03 (dd, 1H, $^2J_{6a,6b}$ = 14.6 Hz, $^3J_{5,6a}$ = 1.5 Hz, H-6^{Ia}), 5.00-4.99 (m, 2H, H-1^{II,B}), 4.97 (d, 1H, $^3J_{1,2}$ = 3.7 Hz, H-1^{I}), 4.83 (d, 1H, ^2J = 12.3 Hz, CH^{a}O, overlapped with HDO), 4.66 (d, 1H, ^2J = 12.3 Hz, CH^{b}O), 4.61 (dd, 1H, $^2J_{6a,6b}$ = 14.6 Hz, $^3J_{5,6b}$ = 9.4 Hz, H-6^{Ib}), 4.21 (dt, ^3J = 9.7 Hz, ^3J = 1.3 Hz, H-5^{I}), 4.05 (dd, 1H, $^3J_{2,3}$ = 3.3 Hz, $^3J_{1,2}$ = 1.8 Hz, H-2^{B}), 4.03-3.92 (m, 8H, H-2^{A},3$^{I,III-VII}$,5^{VII}), 3.90-3.81 (18H, H-3^{II,A,B},4^{B},5^{III-VI},6$^{(III-VII)(a,b)}$), 3.77-3.63 (m, 9H, H-2$^{I,III-VII}$,4^{A},6$^{A(a,b)}$), 3.63-3.54 (m, 9H, H-2^{II},4$^{III-VII}$,5^{A},6$^{B(a,b)}$), 3.54 (t, 1H, ^3J = 10.1 Hz, H-4^{I}), 3.50-3.48 (m, 3H, H-4^{II,5II,B}), 3.14 (d, 1H, $^3J_{6a,6b}$ = 11.2 Hz, H-6^{IIa}), 2.78 (d, 1H, $^3J_{6a,6b}$ = 11.2 Hz, H-6^{IIb}); ^{13}C-RMN (125 MHz, D_2O) δ (ppm) 143.4 (C-4-C_2HN_3), 126.8 (C-5-C_2HN_3), 102.3 (C-1^{B}), 102.0 (C-

425 1^{VII}), 101.9-101.8 (C-1^{II-VI}), 101.3 (C-1^{I}), 97.9 (C-1^{A}), 83.0 (C-4^{I}), 81.2-81.0 (C-$4^{III-VII}$), 80.6 (C-
426 4^{II}), 78.6 (C-2^{A}), 73.2-71.7 (C-2^{I-VII},3^{I-VII},$5^{III-VII,A,B}$), 71.4 (C-5^{II}), 70.5 (C-5^{I}), 70.2 (C-3^{B}), 70.1 (C-
427 3^{A}), 69.9 (C-2^{B}), 66.8 (C-4^{A}), 66.7 (C-4^{B}), 61.0 (C-6^{B}), 60.8 (C-6^{A}), 60.3 (C-6^{VII}), 60.2 (C-6^{III-VI}),
428 59.8 (CH_2O), 59.1 (C-6^{II}), 51.2 (C-6^{I}); MALDI-TOF-MS *m*/*z* calcd for $C_{57}H_{93}N_3O_{45}Na^+$ 1562.5,
429 found 1562.2 $(M + Na)^+$.

430

431 **3. Results and discussion**

432 *3.1. Synthesis*

433 In order to introduce the NOPD 3-(trifluoromethyl)-4-nitrobenzenamine along with a
434 mannose or α(1→2)mannobioside targeting functionality on the primary face of the β-CD, we
435 started from the 6^{I}-monoazido-6^{X}-*N*-{3-[*N'*-(4'-nitro-3'-trifluoromethylphen-1'-
436 yl)amino]propylamino}-β-CD derivative **1** (Scheme 1). We have recently reported the synthesis of
437 **1** as a mixture of regioisomers (Benkovics et al., 2017). Cyclodextrin derivative **1** already carries
438 the desired NOPD moiety as well as an azido group that would allow the attachment of additional
439 appendages through Huisgen [3+2] copper(I)-catalyzed azide–alkyne cycloadditions (CuAACs).
440 Such reaction, which can be performed in water and is fully compatible with unprotected hydroxyl
441 groups, requires the presence of terminal alkyne functions on the structures which is intended to be
442 clicked to the macrocycle (Meldal & Tornøe, 2008). Indeed, the reaction of **1** with propargyl α-D-
443 mannose **3** using CuI as catalyst in a water-DMF mixture afforded **ManNOPDβCD** as a light-
444 sensitive yellow solid in 71% yield after column chromatography and dialysis purification. We
445 observed that this reaction worked better when the catalyst was added as a water suspension on a
446 pre-heated mixture in DMF of **1** and **3**. The structure of **ManNOPDβCD** was first confirmed by
447 ESI-TOF mass spectrometry, which showed only one peak of *m*/*z* corresponding to the expected
448 $[M+H]^+$ ion. Both ^1H and ^{13}C NMR spectra were intricate due to the presence of several
449 regioisomers in the product. However, it was possible to distinguish significant groups of signals
450 which were not present in the starting azide **1** such as a singlet at δ 8.06 ppm in ^1H NMR, as well as
451 two sets of signals at δ 143.5-143.4 and 127.3-126.5 ppm in ^{13}C NMR, that correspond to the 1,2,3-
452 triazole residue that results from the cycloaddition. It should be noted that the resonances of the
453 low-field signals corresponding to the 3-(trifluoromethyl)-4-nitrobenzenamine moiety were still
454 evident in both ^1H and ^{13}C RMN. Taken together, all these data strongly suggested that conjugation
455 of propargyl α-D-mannose **3** had succeeded through the azide present in **1** without altering the rest
456 of the structure of the latter.

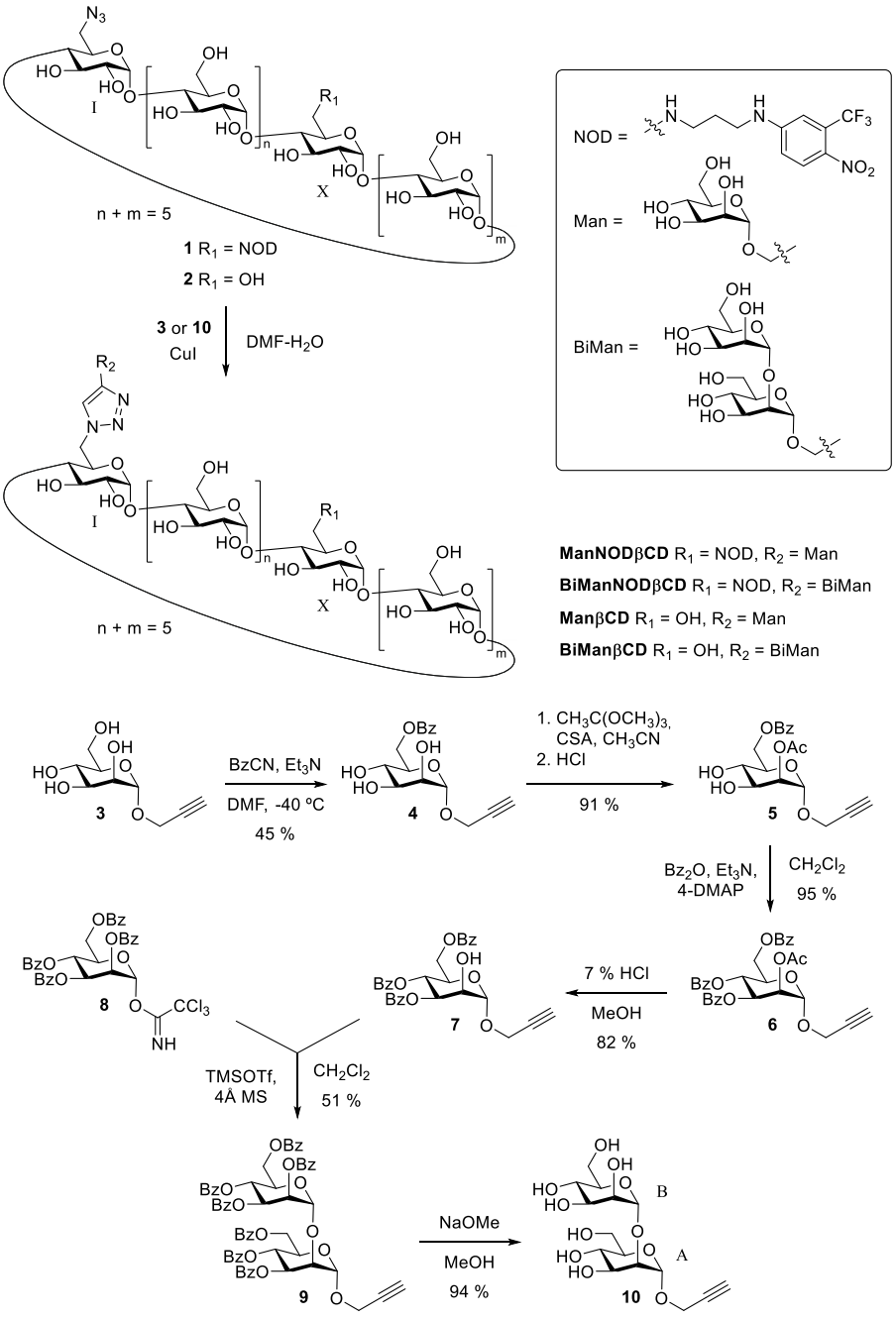

Scheme 1

Next we extended this strategy to the attachment of an α(1→2)mannobioside residue on derivative **1**, as this disaccharide has been reported to be the key moiety of high mannose glycans that define the pathogenicity of a number of viruses and bacteria (Adams et al., 2004). In this regard, we prepared propargyl α-D-mannopyranosyl-(1→2)-α-D-mannopyranoside starting from propargyl α-D-mannose **3** (Scheme 1) according to the methodology recently described by Reina, Di Maio, Ramon-Soriano, Figueiredo & Rojo (2016) for the synthesis of similar α(1→2)mannobiosides. Thus, compound **3** was converted into the 3,4,6-tri-*O*-benzoyl derivative **7** in overall 33% yield after four successive steps: (i) benzoylation of C-6 hydroxyl group (**4**) by treatment with BzCN at -40 ºC in the presence of catalytic amount of Et_3N. These conditions, however, always led to a mixture of products including **4** and other over-benzoylated species that were conveniently isolated by chromatography column; (ii) selective acetylation of C-2 hydroxyl group (**5**) by reaction with trimethyl orthoacetate and camphorsulphonic acid (CSA), followed by

partial hydrolysis of the resulting intermolecular C-2,C-3 orthoester with 1 M aqueous HCl; (iii) benzoylation of remaining C-3 and C-4 hydroxyl groups (**6**) by treatment with Bz_2O, Et_3N and 4-dimethylaminopyridine (4-DMAP); and (iv) deacetylation of C-2 hydroxyl group by using a 7% HCl solution in MeOH. Once prepared, compound **7** was used as acceptor for the mannoside donor **8** using TMSOTf as catalyst to yield **9** in 51% after purification, which was finally deprotected under Zemplén conditions giving the desired propargyl α(1→2)mannobioside **10** in 94%. Both ESI-TOF and NMR data confirmed the structure of **10**. Thus, anomeric protons for A and B mannose moieties gave two doublets at δ 5.27 and 5.02 ppm, respectively. Unequivocal assignation of these signals was carried out by selective 1D ROESY experiments (see supplementary data). In addition, propargylic proton was observed as a triplet at δ 2.91 ppm. Finally, compound **10** was conjugated with azide **1** under the same conditions described above to give **BiManNOPDβCD** in 88% yield after chromatographic purification and dialysis. As in the case of **ManNOPDβCD**, **BiManNOPDβCD** was a mixture of regioisomers and showed complex NMR spectra, although a series of signals suggested that the conjugation had taken place including a singlet at δ 8.06 ppm in ^{1}H NMR, as well as two sets of signals at δ 144.1-144.0 and 127.7-126.0 ppm in ^{13}C NMR corresponding to the triazole linkage.

Finally, as model compounds to estimate the effect of the presence of the NOPD moiety we also prepared **ManβCD** and **BiManβCD** by reaction of 6^I-azido-6^I-deoxy-β-cyclodextrin **2** with propargyl derivatives **3** or **10** (Scheme 1) under the same conditions already indicated for the preparation of the NOPD-containing analogues. **ManβCD** and **BiManβCD** were obtained in 92 and 90% yield, respectively, after column chromatography. Since these compounds were regioisomerically pure their NMR spectra were much simpler. Indeed, apart from those signals indicating the formation of the 1,2,3-triazole spacer located around δ 8.10 ppm in ^{1}H NMR and δ 143.4 and 123.8 ppm in ^{13}C NMR, it was possible to observe the anomeric protons of those mannose moieties directly linked to the spacer, as doublets at δ 5.02 and 5.21 ppm for **ManβCD** and **BiManβCD**, respectively. These two signals allowed the unequivocal assignment of the rest of signals belonging to the mannose residues and the glucose appended with the linker through selective 1D TOCSY and 1D ROESY, as well as 2D HSQC, experiments (see supplementary data). MALDI-TOF-MS also confirmed the structure of these compounds as *m*/*z* peaks corresponded to the correct $[M+Na]^+$ ions for each one.

3.2. Supramolecular behavior

It is well known that the NOPD 3-(trifluoromethyl)-4-nitrobenzenamine moiety can be accommodated within the cavity of β-CD in aqueous solutions forming 1:1 complexes with an estimated binding constant (*K*) between 200 ± 16 and 300 ± 50 M^{-1} (Taraszewska, Migut, & Koźbiał, 2003). This fact made us envisage that **ManNOPDβCD** and **BiManNOPDβCD**, both presenting simultaneously a chromophore moiety and a β-CD macrocycle, would probably undergo self-aggregation processes in water. This hypothesis was first tested by 2D ROESY NMR spectra in deuterated water (see Figure 1 and supplementary data). As can be seen, clear NOE cross-peaks were found between the three groups of low-field signals at δ 8.32-8.22, 8.16-8.11 and 6.97-6.90 ppm belonging to the aromatic protons of the chromophore, and those multiplets appearing at δ 4.29-3.16 ppm where H-3 and H-5 protons located at the inner wall of the CD cavity are overlapped. These results strongly suggested the inclusion of the NOPD inside the central hole of the macrocycle (Casas-Solvas et al., 2009). However, the complexity of the ^{1}H NMR spectra of these conjugates due to the presence of several regioisomers made difficult to propose any inclusion

geometry for the self-complexation. Although molecular modeling has indicated that the 3-(trifluoromethyl)-4-nitrobenzenamine moiety in the anti-androgen drug flutamide can enter the β-CD cavity through the secondary face protruding the NO_2 group through the primary rim (Taraszewska, Migut, & Koźbiał, 2003), to the best of our knowledge there is not any experimental evidence that support such spatial arrangement. Furthermore, ICD experiments suggested that more than one complex geometry might simultaneously occur during this interaction (Sortino et al., 2001). Consequently, at least three different self-inclusion modes could be proposed to explain the referred NOE cross-peaks in 2D ROESY NMR experiments measured for **ManNOPDβCD** and **BiManNOPDβCD** in water (Figure 2). Thus, the 3-(trifluoromethyl)-4-nitrobenzenamine moiety may undergo a monomeric intramolecular inclusion within the cavity through the primary face of the macrocycle if the trimethyldiamine linker was long and flexible enough to achieve this layout (structure A in Figure 2). In addition, one could envisage the formation of a head-to-head homodimer due to the interpenetration of the NOPD residues into the facing macrocycle cavities through their primary openings (structure B). The advantage of this spatial arrangement is the simultaneous cooperative participation of the two CD moieties, which might be crucial for the stability of the aggregation taking into account the low values on the binding constant estimated for the interaction of the 3-(trifluoromethyl)-4-nitrobenzenamine moiety with native β-CD. Finally, a linear supramolecular assembly involving *n* conjugate molecules could also be proposed considering the penetration of the NOPD residue of each molecule into the cavity of the following one through its secondary face in a head-to-tail fashion (structure C).

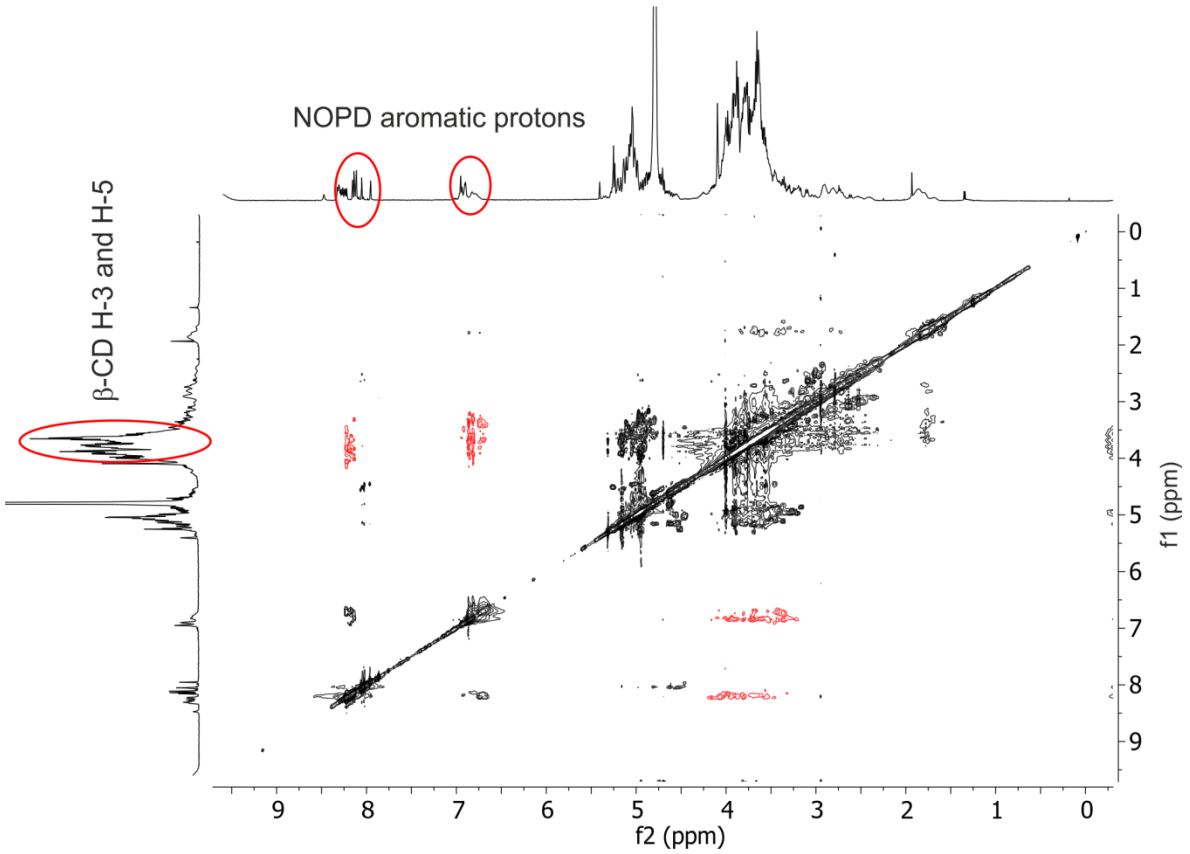

Figure 1. 2D-ROESY spectrum in D_2O with WATERGATE (600 MHz, 25 ºC, 200 ms of mixing time) for **BiManNOPDβCD**. Cross-picks between the aromatic protons of the nitroaniline and the inner H-3 and H-5 protons of the β-CD are displayed in red.

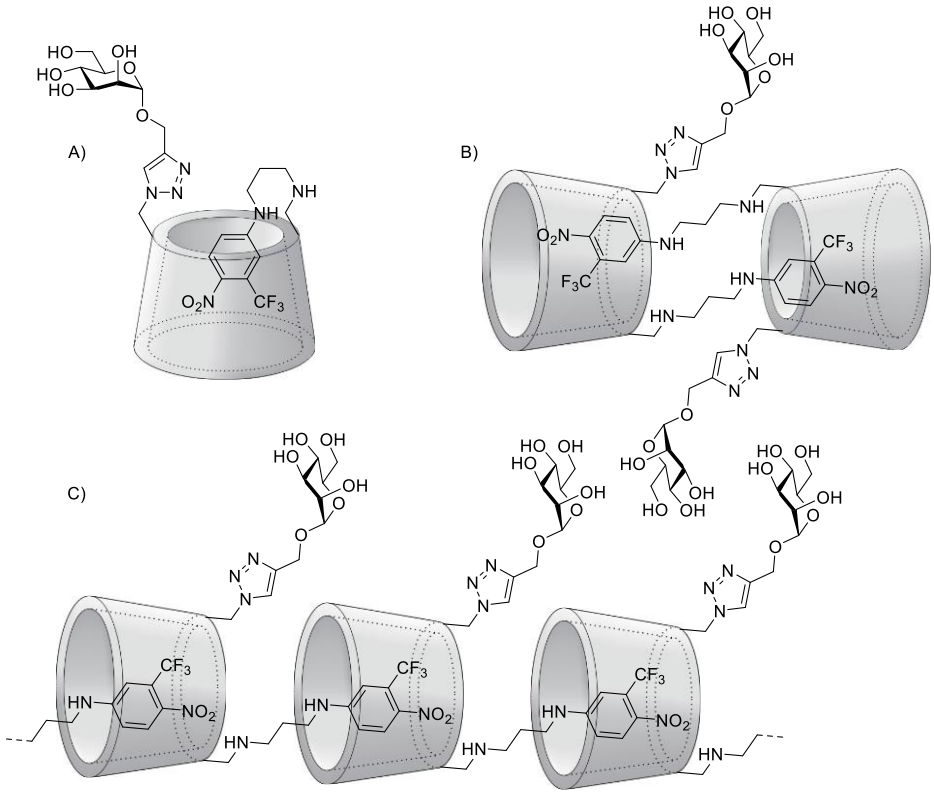

Figure 2. Proposed structures for the supramolecular self-inclusion process of **ManNOPDβCD** in water, which could be extended also for **BiManNOPDβCD**. A) Monomeric intramolecular self-inclusion. B) Head-to-head dimeric interpenetration through the primary face of the macrocycle. C) Head-to-tail polymeric self-aggregation through the secondary face of the macrocycle.

Assuming that each structure depicted in Figure 2 would lead to significantly different hydrodynamic diameters (d_H), we tried to gain insight into the self-aggregation structures of **ManNOPDβCD** and **BiManNOPDβCD** by comparing their d_H values in D_2O with those for β-CD, **ManβCD** and **BiManβCD** obtained by pulse-gradient stimulated echo (PGSE) NMR experiments (Pregosin et al., 2005; Macchioni et al., 2008). Measured *D* values (Table 1) were used to estimate the corresponding d_H of the diffusing species by using the Stokes-Einstein equation assuming a spherical geometry for β-CD, **ManβCD** and **BiManβCD**, and a prolate spheroid shape for **ManNOPDβCD** and **BiManNOPDβCD**. In addition, the D_2O viscosity value was assumed to be constant, although it varies with the concentration of cyclodextrin derivatives, and equal to that reported for H_2O. Thus, it is important to point out that such assumptions might render inaccurate estimation of the hydrodynamic diameters, which should be, in turn, considered as apparent. The *D* value obtained for native β-CD was 2.72 x 10^{-10} m^2 s^{-1}, which involved a d_H of 1.78 nm. Such *D* value is in close agreement with those (2.64-2.71 x 10^{-10} m^2 s^{-1}) previously reported for this cyclooligosaccharide when using the same technique (Guerrero-Martínez, González-Gaitano, Viñas, & Tardajos, 2006; Cabaleiro-Lago, Nilsson, Valente, Bonini, & Söderman, 2006). Diffusion coefficients for **ManβCD** and **BiManβCD** (2.64 and 2.36 x 10^{-10} m^2 s^{-1}, respectively) decreased 3% and 15%, respectively, as compared with β-CD, which indicated a slight increment of the molecular size (d_H of 1.84 and 2.04 nm, respectively) consistent with the presence of an appended mannoside or α(1→2)mannobioside moiety, respectively.

Table 1. Diffusion coefficients (D) and hydrodynamic diameters (d_H) values for β-CD, **ManβCD**, **BiManβCD**, **ManNOPDβCD** and **BiManNOPDβCD** (10 mM) obtained by PGSE NMR at 20 ºC in D_2O

Compound	D x 10^{10} (m^2 s^{-1})[a]	Sphere	Prolate spheroid	
		d_H (nm)[b]	Minor axes (nm)[c]	Major axes (nm)[d]
β-CD	2.72	1.78		
ManβCD	2.64	1.84		
BiManβCD	2.36	2.04		
ManNOPDβCD	2.20	2.20	1.84	3.14
BiManNOPDβCD	1.95	2.48	2.04	3.66

[a]The experimental error in the D values is ±2%. [b]Obtained from the Stokes-Einstein equation assuming a spherical geometry and the water viscosity η(H_2O) to be constant and equal to 0.890 x 10^{-3} kg m^{-1} s^{-1} (www.knovel.com). [c]Fixed as the d_H of the **ManβCD** and **BiManβCD** analogues. [d]Calculated from the volume of the equivalent sphere.

In sharp contrast, the presence of the NOPD moiety on **ManNOPDβCD** and **BiManNOPDβCD** analogues led to D values 24% and 39% smaller than that for β-CD, suggesting that an aggregation process might take place. In a case like this, in which two conjugate molecules are forming a supramolecular self-inclusion dimer, a prolate spheroid model of the same volume as that for the equivalent sphere calculated from the Stokes-Einstein equation would be more adequate to represent the actual shape of the aggregate. Considering that the NOPD moieties would be within the β-CD cavities in such structure, we can assume that the minor axes of the spheroid representing the self-associated head-to-head or head-to-tail structures of **ManNOPDβCD** and **BiManNOPDβCD** equal the d_H values estimated for **ManβCD** and **BiManβCD**. Interestingly, this model depicted minimum major axis for the spheroids describing **ManNOPDβCD** and **BiManNOPDβCD** of 3.14 and 3.66 nm, respectively, which turned out to be 1.71 and 1.79-fold larger than d_H values for **ManβCD** and **BiManβCD**. These results strongly suggested that **ManNOPDβCD** and **BiManNOPDβCD** preferentially formed head-to-head homodimeric structure B in water (Figure 2), although monomeric self-inclusion (structure A) and head-to-tail dimer C containing only two molecules cannot be dismissed and might also occur to a lesser extent.

3.3. ConA binding affinity studies by ITC

The presence of mannose and α(1→2)mannobioside moieties on **ManNOPDβCD** and **BiManNOPDβCD** endow these conjugates with targeting functionalities towards pathogens showing mannose-receptor lectins on their surface. To test the biorecognition abilities of such conjugates, we used concanavalin A (ConA) lectin from *Canavalia ensiformis* (Jack bean) as a well-known model of mannose-specific lectins (Casas-Solvas et al., 2008). The non-containing-NOPD analogues **ManβCD** and **BiManβCD** were also used in this study for comparative purposes. Binding studies were carried out by isothermal titration calorimetry (ITC), as this technique is well-known to provide a full thermodynamic profile of the interaction. Indeed, the observed enthalpy change of binding (ΔH) is directly measured from the thermogram, and both the binding constant (K) and the stoichiometry (n, which represents the [conjugate]:[ConA] ratio when the lectin binding sites are fully saturated) are then estimated by using a nonlinear least square algorithm to fit the data to a model of equal and independent binding sites, as this lectin has been reported to present a single carbohydrate-binding site per monomer (Dam & Brewer, 2002).

Titration experiments were performed by injecting aliquots of solutions of each conjugates into the calorimeter cell containing a solution of the lectin. Thermograms for each conjugate were obtained by plotting heat released or absorbed after each injection against [conjugate]-[ConA] molar ratio (see Figure 3 and supplementary data). Thermodynamic parameters for each interaction are given in Table 2 and Figure 4.

Table 2. Thermodynamics and stability constants for the binding of conjugates **ManβCD**, **BiManβCD**, **ManNOPDβCD** and **BiManNOPDβCD** to ConA in 20 mM phosphate buffer (pH 7.2) containing 20 mM NaCl, 100 μM $CaCl_2$ and 100 μM $MnCl_2$ at 25 ºC (*n* equal and independent binding sites model).

Conjugate	n^a	K (M^{-1})	ΔG^0 (kcal mol^{-1})	ΔH (kcal mol^{-1})	$T\Delta S^0$ (kcal mol^{-1})
Me α-D-Man[b]	1.00	7600±228	-5.29±0.02	-6.80±0.10	-1.51±0.10
ManβCD	1.10±0.02	9120±356	-5.40±0.02	-7.40±0.13	-2.00±0.13
BiManβCD	1.10±0.01	111000±2200	-6.88±0.01	-8.46±0.03	-1.58±0.03
ManNOPDβCD	1.25±0.06	15700±1130	-5.72±0.04	-3.65±0.20	2.07±0.20
BiManNOPDβCD	1.07±0.01	175000±11400	-7.15±0.04	-7.23±0.08	-0.08±0.09

[a][conjugate]:[ConA] ratio when the lectin binding sites are fully saturated; [b]Chervenak & Toone, 1995.

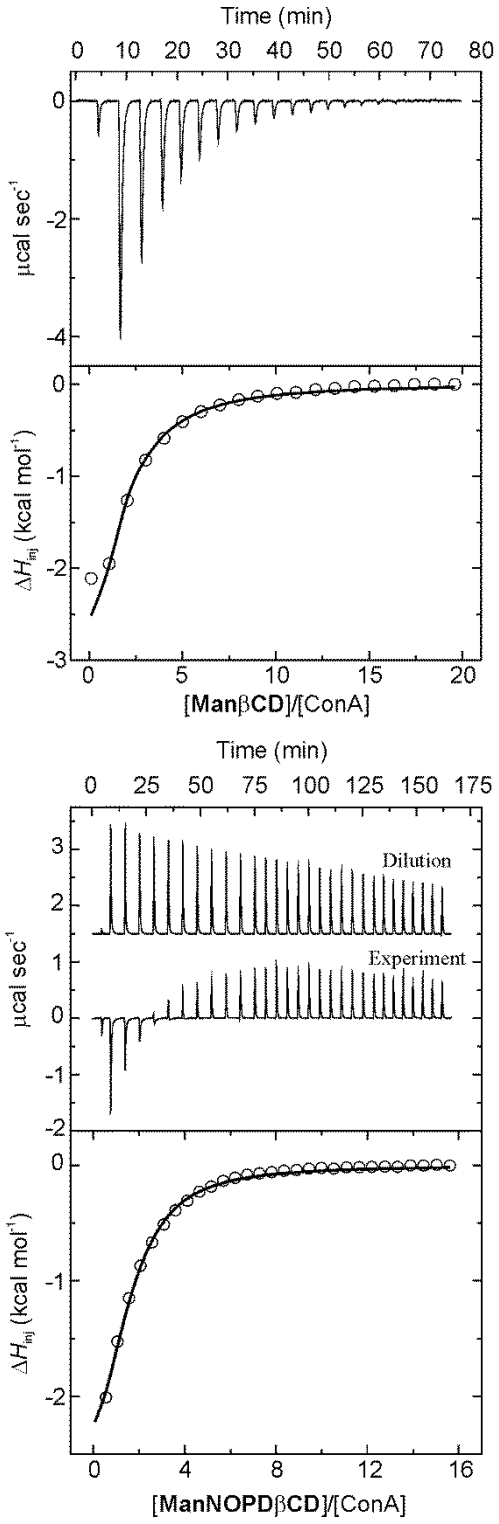

611

612 Figure 3. Titration of ConA with **ManβCD** (top) and **ManNOPDβCD** (bottom) in 20 mM
613 phosphate buffer (pH 7.2) containing 20 mM NaCl, 100 µM $CaCl_2$ and 100 µM $MnCl_2$ at 25 ºC.
614 The top panels show the raw calorimetric data indicating the amount of exchanged heat for each
615 injection of **ManβCD** or **ManNOPDβCD**. The area under each peak corresponds to the heat
616 amount released or absorbed upon binding of the mannosylated βCD to the lectin. As the titrations
617 progress the area under the peaks gradually becomes smaller because of the increasing saturation of
618 the sugar binding sites of the protein. Such area was integrated and plotted against the molar ratio of
619 the βCD derivative to ConA (as monomer). The smooth solid lines represent the best fit of the
620 experimental data to the model of *n* equal and independent binding sites.

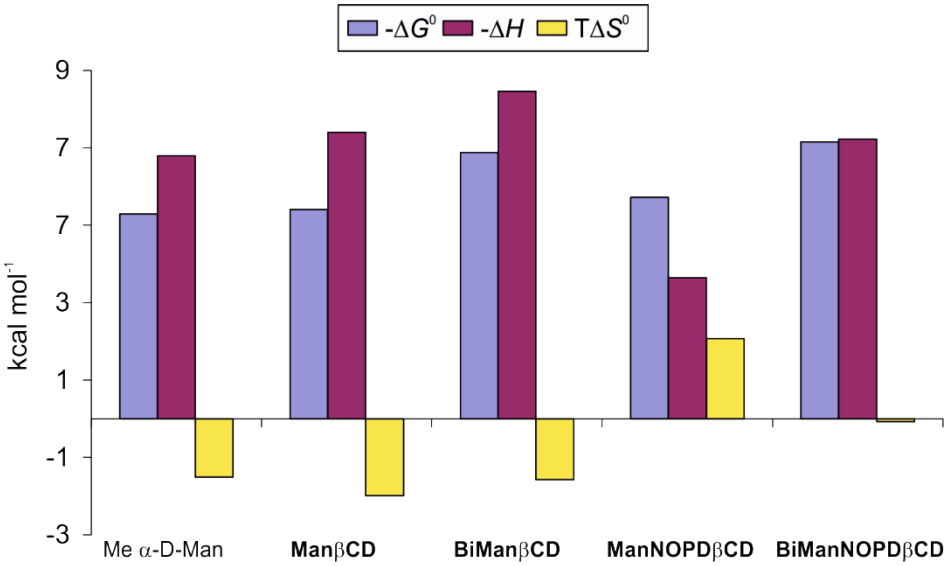

Figure 4. Thermodynamic profiles including free energy ($-\Delta G^0$), enthalpy ($-\Delta H$), and entropy changes ($T\Delta S^0$) for the binding of conjugates **ManβCD**, **BiManβCD**, **ManNOPDβCD** and **BiManNOPDβCD** to ConA in 20 mM phosphate buffer (pH 7.2) containing 20 mM NaCl, 100 μM $CaCl_2$ and 100 μM $MnCl_2$ at 25 ◦C.

As can be seen, the interaction of conjugates **ManβCD** and **BiManβCD** lacking NOPD moieties is clearly exothermic. The corresponding thermograms present a set of negative peaks indicating a heat release after each injection which becomes smaller as the titration successes. Thermodynamic profiles are enthalpy-driven in both cases, with large negative (i.e. favorable) enthalpic contributions partially compensated by smaller negative (i.e. unfavorable) entropic terms. This behavior has been reported as typical energetics of protein–carbohydrate associations (Casas-Solvas et al., 2008). Indeed, thermodynamic data for the interaction of methyl α-D-mannoside (Me α-D-Man) with ConA (Chervenak & Toone, 1995) are given for comparison (Table 2 and Figure 4). In fact, *K* values for Me α-D-Man and **ManβCD** (7600 and 9120 M^{-1}, respectively) are very similar, indicating that the presence of the triazole linker and the β-CD macrocycle at the anomeric position of the sugar do not have any significant effect on the association with the lectin. In the case of **BiManβCD**, however, the binding constant (111000 M^{-1}) turned out to be 12-fold stronger than that for **ManβCD**, which implies that α(1→2)mannobioside residue is a far better ligand for ConA lectin than the mannose monosaccharide. Such increased avidity arises from a 14% more favorable enthalpic contribution along with a 21% less unfavorable entropic factor, which may be reasoned in terms of a better fit of the α(1→2)mannobioside moiety within the carbohydrate-binding site of the protein.

Interestingly, the presence of the NOPD appendage on **ManNOPDβCD** and **BiManNOPDβCD** sharply modifies the thermodynamic profiles of association to ConA leading to a much more complex behavior (see Figure 3 and supplementary data). Thus, although negative exothermic peaks initially appeared, they quickly became positive (i. e. endothermic) after a few injections until reached a plateau and began to decrease gradually. This behavior was especially evident for **ManNOPDβCD**, although it also succeeded in the case of **BiManNOPDβCD**. These data suggested that two different processes seemed to occur simultaneously. Indeed, dilution processes for these two conjugates were clearly endothermic showing intensity that decreased along the experiment while their analogues **ManβCD** and **BiManβCD** not presenting NOPD moieties gave negligible dilution peaks. Such results might be due to the disassembly of self-aggregates

during dilution (Casas-Solvas et al., 2009), although depletion was linear and thus could not be fitted to any dissociation model. In any case, it is clear that this endothermic dilution feature compensates the exothermic binding event of the sugar appendage to the lectin. Initially, the latter process is more energetic and dominates the thermogram, given neat negative peaks. However, as the experiment progresses, binding becomes less intense probably due to the increasing saturation of the sugar binding sites of the protein and endothermic dilution gradually takes control on the resulting peaks. As a result, thermodynamic parameters obtained for **ManNOPDβCD** and **BiManNOPDβCD** would contain information about both events and thus should be considered as apparent.

As can be seen from Table 2 and Figure 4, thermodynamic profiles for the interaction of **ManNOPDβCD** and **BiManNOPDβCD** steeply differ from those previously discussed for **ManβCD** and **BiManβCD**. Although both are still enthalpy-driven, in the case of **ManNOPDβCD** enthalpic term also contributes favorably in 36% to the binding, suggesting that a more efficient dehydration might take place. In consequence, despite the fact that this conjugate shows a ΔH value 49% smaller than that for its **ManβCD** analogue, the binding constant turned out to be 1.7-fold stronger. It is difficult to unequivocally explain this behavior, but it might be due to a multivalent effect of the carbohydrate caused by the homodimerization process suggested by NMR and DLS data. However, it should not be discounted that the aromatic moiety may somehow take part in the binding process with the protein, since it is well known that many lectins possess hydrophobic binding sites, in particular around the site where aglycon groups would localize upon carbohydrate–lectin complexation (Casas-Solvas et al., 2008). Similarly, **BiManNOPDβCD** gave a K value 1.6-fold larger than that found for the conjugate **BiManβCD**, although in this case the entropic term was almost negligibly unfavorable and contributed less than 1% to the free energy change of the binding. As can be seen from the thermograms (see Figure 3 and supplementary data), the endothermic dilution process is less intense for **BiManNOPDβCD** as compared to **ManNOPDβCD**, and thus seems not to be enough to fully compensate the negative entropy change that arises from the simple interaction of the carbohydrate moiety observed for **BiManβCD**. In any case, it is clear that the presence of NOPD residue on both **ManNOPDβCD** and **BiManNOPDβCD** clearly increases the avidity of ConA for these conjugates.

3.4. Spectroscopic and photochemical behavior

The absorption spectra of **ManNOPDβCD** and **BiManNOPDβCD** together with that of N-(3-aminopropyl)-3-(trifluoromethyl)-4-nitrobenzenamine chosen as suitable model compound are shown in Figure 5. As expected, the spectral profiles of the CD derivatives are dominated by the dominant absorption of the nitroaniline moiety (Caruso, Petralia, Conoci, Giuffrida, & Sortino, 2007). However, a small but indicative blue shift of the absorption maxima (ca. 7 nm) for both **ManNOPDβCD** and **BiManNOPDβCD** with respect to the model compound is observed (see later). Such a shift is in line with the supramolecular behavior and can be due to lower polarity of the CD cavity experienced by the nitroaniline chromophore upon formation of the inclusion complexes. In fact, due to the large difference of the dipole moments between the ground and first π,π^* state responsible for the first large absorption band (Sortino et al. 2001), one would expect a blue shift of this band going from water to a less polar solvent.

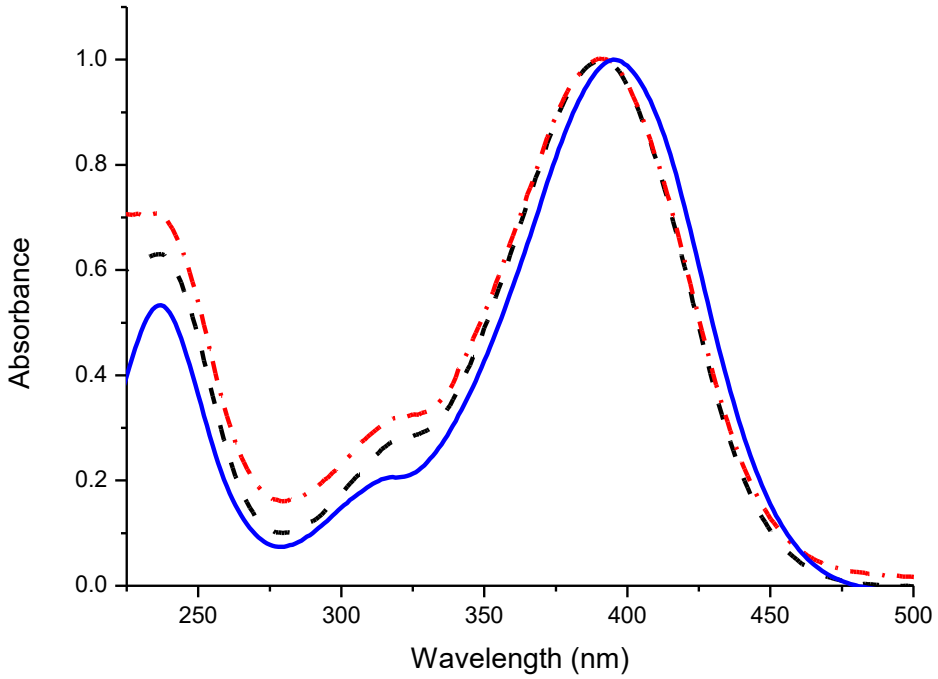

Figure 5. Normalized absorption spectra in aqueous solution of **ManNOPDβCD** (dashed), **BiManNOPDβCD** (dashed-dotted) and N-(3-aminopropyl)-3-(trifluoromethyl)-4-nitrobenzenamine (solid)

The NO delivery capability of the CD derivatives under light stimuli was investigated using an ultrasensitive NO electrode for the direct and real-time monitoring of this transient species. Such electrode directly reveals NO with high sensitivity (nM concentrations) by an amperometric technique (Coneski and Schoenfisch, 2012). Optically matched aqueous solutions of **ManNOPDβCD** and **BiManNOPDβCD** and, for comparison, the model compound, were subjected to alternate cycles of light (λ_{exc} = 405 nm) and dark. The results illustrated in Figure 6 provide unambiguous evidence that both **ManNOPDβCD** and **BiManNOPDβCD** are very stable in the dark and supply NO exclusively under irradiation with visible light. Note that, the rate of photorelease is very similar for both the CD derivatives and higher than that observed for the model compound. This increased NO photodelivery efficiency is not surprising and can be due to an active role of the CD cavity which act as a nanoreactor that provides a low polarity environment and abstractable hydrogens nearby the phenoxy radical intermediate involved in the NO photorelease mechanism (see Caruso, Petralia, Conoci, Giuffrida, & Sortino, 2007). A similar behavior has been already observed for this NOPD encapsulated in micelles of Pluronic (Taladriz-Blanco, 2014) and amphiphilic calixarenes (Di Bari, 2016).

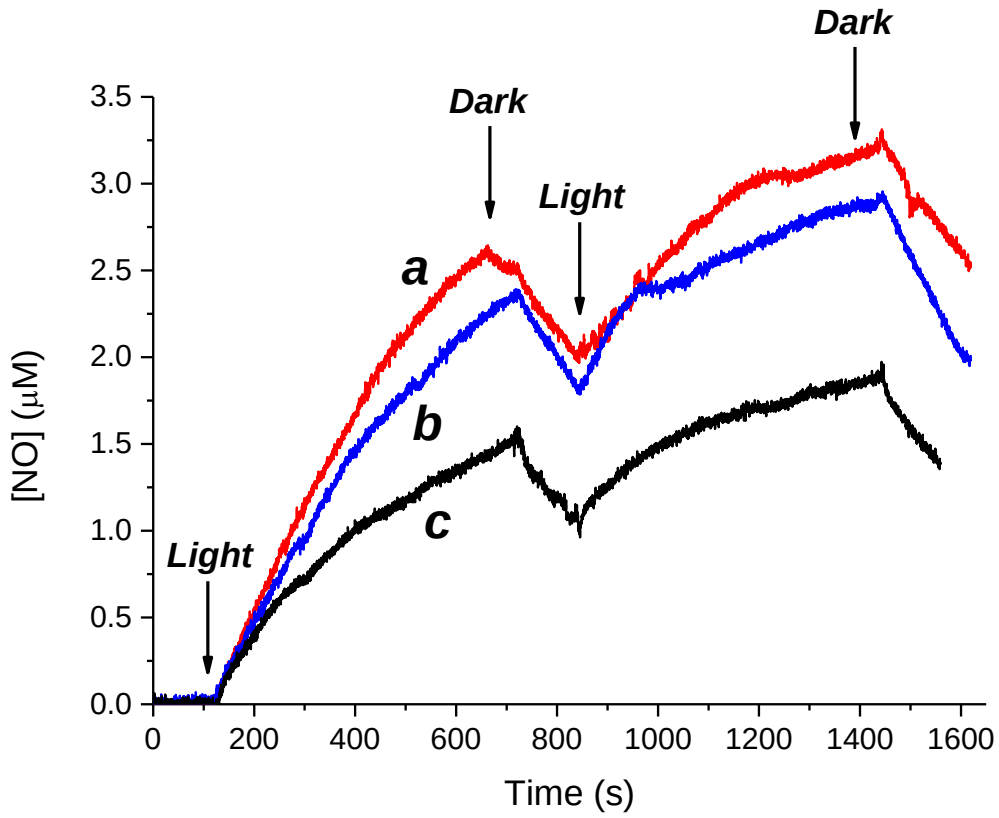

Figure 6. NO release profile observed for 80 μM aqueous solutions of **ManNOPDβCD** (***a***) and **BiManNOPDβCD** (***b***) and an optically matched aqueous solution of the model compound N-(3-aminopropyl)-3-(trifluoromethyl)-4-nitrobenzenamine (***c***). λ_{exc} = 405 nm

4. Conclusions

In summary, we have synthesized two new β-CD derivatives containing on their primary face two randomly appended functional moieties: a) a NO photodonor 4-nitro-3-(trifluoromethyl)aniline group, and b) a mannose or α(1→2)mannobioside residue as targeting functionalities to provide the conjugates with avidity for mannose-binding lectins. Both bifunctional cyclooligomers were found to be fully soluble in water. As initially hypothesized, the conjugates underwent supramolecular self-aggregation processes due to the self-inclusion of the NOPD moiety within the β-CD cavity. In particular, 2D ROESY and PGSE NMR experiments suggested that they formed supramolecular head-to-head homodimers that might occur by the interpenetration of the nitroaniline residues into the facing macrocycle cavities through their primary openings. The bio-recognition abilities of the conjugates were tested towards concanavalin A lectin by isothermal titration calorimetry. Thermograms were complex since at least two different thermodynamic processes took place: an exothermic lectin binding event and an endothermic process during the dilution of the conjugates that might be reasoned in terms of aggregates disassembly. It was found that α(1→2)mannobioside moiety provided lectin binding constants two orders of magnitude larger than that for mannose residue. In addition, the presence of nitroaniline enhanced the binding interaction with ConA between 1.6 and 1.7 times with respect to the non-containing-nitroaniline analogue structures. This effect might be due to the multivalent effect of the carbohydrate caused by homodimerization. Despite the formation of supramolecular structures both CD derivatives are able to release NO under the control of visible light with efficiency even higher than that of the

unfunctionalized NOPD unit. In this regard, the CD cavity as a nanoreactor with reduced polarity and presence of easily abstractable H-atom, indispensable in the mechanism of the NO photorelease, is envisaged to play a key role.

Acknowledgements

The authors acknowledge the Spanish Ministry of Economy and Competitiveness (Grants CTQ2013-48380-R and CTQ2017-900-50R) and the European Union through FP7-PEOPLE-2013-ITN (http://itn-cyclonhit.eu) project (Grant Agreement no. 608407)

Appendix A. Supplementary data

Supplementary data associated with this article can be found, in the online version, at (to be completed when accepted)

References

Adams, E. W., Ratner, D. M., Bokesch, H. R., McMahon, J. B., O'Keefe, B. R., & Seeberger, P. H. (2004). Oligosaccharide and glycoprotein microarrays as tools in HIV glycobiology: glycan-dependent gp120/protein interactions, Chemistry & Biology, 2004, 11(6), 875-881. http://dx.doi.org/10.1016/j.chembiol.2004.04.010

Bausanne, I., Benito, J. M., Ortiz Mellet, C., García Fernandez, J. M., Law, H., & Defaye, J., (2000). Synthesis and comparative lectin-binding affinity of mannosyl-coated β-cyclodextrin-dendrimer constructs, *Chemical Communication*, *2000*(16), 1489-1490. http://dx.doi.org/10.1039/b003765f

Benito, J. M., Gomez-García, M., Ortiz Mellet, C., Bausanne, I., Defaye, J., & García Fernandez, J. M. (2004). Optimizing saccharide-directed molecular delivery to biological receptors: design, synthesis, and biological evaluation of glycodendrimer−cyclodextrin conjugates. *Journal of the American Chemical Society*, *126*(33), 10355-10363. http://dx.doi.org/10.1021/ja047864v

Benkovics, G., Perez-Lloret, M., Afonso, D., Darcsi, A., Béni, S., Fenyvesi, E., et al. (2017). A multifunctional β-cyclodextrin conjugate photodelivering nitric oxide with fluorescence reporting. *International Journal of Pharmaceutics*, *531*(2), 614-620. https://dx.doi.org/10.1016/j.ijpharm.2017.05.023

Cabaleiro-Lago, C., Nilsson, M., Valente, A. J. M., Bonini, M., & Söderman, O. (2006). NMR diffusometry and conductometry study of the host–guest association between β-cyclodextrin and dodecane 1,12-bis(trimethylammonium bromide). *Journal of Colloid and Interface Science*, *300*(2), 782-787. http://dx.doi.org/ 10.1016/j.jcis.2006.04.016

Carpenter, A. W., & Schoenfisch, M. H. (2012). Nitric oxide release: Part II. Therapeutic applications, *Chemical Society Reviews*, *41*(10), 3742-3752. http://dx.doi.org/10.1039/c2cs15273h

Caruso, E. B., Petralia, S., Conoci, S., Giuffrida, S., & Sortino, S. (2007). Photodelivery of nitric oxide from water-soluble platinum nanoparticles. *Journal of the American Chemical Society, 129*(3), 480-481. http://dx.doi.org/10.1021/ja067568d

Casas-Solvas, J. M., Ortiz-Salmerón, E., García-Fuentes, L., & Vargas-Berenguel, A. (2008) Ferrocene–mannose conjugates as electrochemical molecular sensors for concanavalin A lectin. *Organic and Biomolecular Chemistry*, *6*(22), 4230-4235. http:/dx.doi.org/10.1039/b809542f

Casas-Solvas, J. M., Ortiz-Salmerón, E., Fernández, I., García-Fuentes, L., Santoyo-González, F., Vargas-Berenguel, A. (2009). Ferrocene–β-cyclodextrin conjugates: cynthesis, cupramolecular behavior, and use as electrochemical sensors. *Chemistry – A European Journal*, *15*(33), 8146-8162. http://dx.doi.org/10.1002/chem.200900593

Casas-Solvas, J. M., & Vargas-Berenguel, A. (2016). Glycoclusters and their applications as anti-infective agents, vaccines, and targeted drug delivery systems. In K. J. Stine (Ed.), Carbohydrate Nanotechnology (Chapter 7, pp. 175-210). Hoboken: John Wiley & Sons, Inc. http://dx.doi.org/10.1002/9781118860212.ch7

Chervenak, M. C., & Toone, E. J. (1995). Calorimetric analysis of the binding of lectins with overlapping carbohydrate-binding ligand specificities. *Biochemistry*, *34*(16), 5685-5695. http://dx.doi.org/ 10.1021/bi00016a045

Cohen, M. L., (2000). Changing patterns of infectious disease, *Nature*, *406*(6797), 762-767. http://dx.doi.org/10.1038/35021206

Coneski, P. N., & Schoenfisch, M. H. (2012). Nitric oxide release: Part III. Measurement and reporting. *Chemical Society Reviews*, *41*(10), 3753-3758. http://dx.doi.org/ 10.1039/c2cs15271a

Conoci, S., Petralia, S., & Sortino, S. (2006). Use of nitroaniline derivatives for the production of nitric oxide. Patent US 8766006 B2

Cutrone, G., Casas-Solvas, J. M., & Vargas-Berenguel, A. (2017). Cyclodextrin-Modified inorganic materials for the construction of nanocarriers, *International Journal of Pharmaceutics*, *531*(2), 621-639. http://dx.doi.org/10.1016/j.ijpharm.2017.06.080

Dam, T. K., & Brewer, F. (2002). Thermodynamic studies of lectin−carbohydrate interactions by isothermal titration calorimetry. *Chemical Reviews*, *102*(2), 387.430. http://dx.doi.org/ 10.1021/cr000401x

Di Bari, I., Picciotto, R., Granata, G., Blano, A. R., Consoli, G. M. L., & Sortino, S. (2016). A bactericidal calix[4]arene-based nanoconstruct with amplified NO photorelease, *Organic & Biomolecular Chemistry*, *14*(34), 8047-8052. http://dx.doi.org/10.1039/c6ob01305h

Duchêne, D., & Bochot, A. (2016). Thirty years with cyclodextrins. *International Journal of Pharmaceutics*, *514*(1), 58-72. http://dx.doi.org/10.1016/j.ijpharm.2016.07.030

Erdmann, R. S., & Wennemens, H. (2010). Functionalizable collagen model peptides. *Journal of the American Chemical Society*, *132*(40), 13957-13959. http://dx.doi.org/10.1021/ja103392t

Figdor, C. G., van Kooyk, Y., & Adema, G. J. (2002). C-type lectin receptors on dendritic cells and langerhans cells, *Nature Reviews Immunology*, *2*(2), 77–84. http://dx.doi.org/10.1038/nri723

Fraix, A., Marino, N., & Sortino, S. (2016). Phototerapeutic release of nitric oxide with engineered nanoconstructs. In S. Sortino (Ed.), *Light-Responsive Nanostructured Systems for Applications in Nanomedicine*, Topics in Current Chemistry, 370 (pp. 225-257). Heidelberg: Springer International Publishing Switzerland. http://dx.doi.org/10.1007/978-3-319-22942-3_8

Gade, M., Khandelwal, P., Sangabathuni, S., Bavireddi, H., Murthy, R. V., Poddar, P., et al. (2016). Immobilization of multivalent glycoprobes on gold surfaces for sensing proteins and macrophages. *Analyst*, *141*(7), 2250-2258. http://dx.doi.org/10.1039/c5an02336j

Guerrero-Martínez, A., González-Gaitano, G., Viñas, M. H., & Tardajos, G (2006). Inclusion complexes between β-cyclodextrin and a gemini surfactant in aqueous solution: an NMR study. *Journal of the Physical Chemistry B*, *110*(28), 13819-13828. http://dx.doi.org/ 10.1021/jp0615813

Halpenny, G. M., & Mascharak, P. K. (2010). Emerging antimicrobial applications of nitric nxide (NO) and NO-releasing materials, *Anti-Infective Agents in Medicinal Chemistry*, *9*(4), 187-197. http://dx.doi.org/10.2174/187152110794785086

Hartmann, M., Betz, P., Sun, Y., Gorb, S. N., Lindhorst, T. K., & Krueger, A. (2012). Saccharide-modified nanodiamond conjugates for the efficient detection and removal of pathogenic bacteria. *Chemistry – A European Journal*, *18*(21), 6485-6492. http://dx.doi.org/10.1002/chem.201104069

Laxminarayan, R., Duse, A., Wattal, C., Zaidi, A. K. , Wertheim, H. F., Sumpradit, N., et al.(2013). Antibiotic resistance-the need for global solutions, *The Lancet Infectious Diseases Commision*, *13*(12), 1057-1098. http://dx.doi.org/10.1016/S1473-3099(13)70318-9

Macchioni, A., Ciancaleoni, G., Zuccaccia, C., & Zuccaccia, D. (2008). Determining accurate molecular sizes in solution through NMR diffusion spectroscopy. *Chemical Society Reviews*, *37*(3), 479-489. http://dx.doi.org/10.1039/b615067p

Magiorakos, A.-P., Srinivasan, A., Careyb, R. B., Carmelic, Y., Falagasde, M. E., Giskef, C. G., et al. (2012). Multidrug-resistant, extensively drug-resistant and pandrug-resistant bacteria: an international expert proposal for interim standard definitions for acquired resistance. *Clinical Microbiology and Infection*, *18*(3), 268-281. http://dx.doi.org/10.1111/j.1469-0691.2011.03570.x

Mazzaglia, A., Sciortino, M. T., Kandoth, N., & Sortino, S. (2012). Cyclodextrin-based nanoconstructs for photoactivated therapies. *Journal of Drug Delivery Science and Technology*, *22*(3), 235-242. http://dx.doi.org/10.1016/s1773-2247(12)50034-1

Meldal, M., & Tornøe, C. W. (2008). Cu-catalyzed azide-alkyne cycloaddition. *Chemical Reviews*, *108*(8), 2952–3015. http://dx.doi.org/10.1021/cr0783479.

Perrin, D. D., & Armarego, W. F. L. (1989). *Purification of Laboratory Chemicals*. (3rd ed.). Oxford: Pergamon.

Poláková, M., Beláňová, M., Mikušová, K., Lattová, E., & Perreault, H. (2011). Synthesis of 1,2,3-triazolo-linked octyl (1→6)-α-D-oligomannosides and their evaluation in mycobacterial mannosyltransferase assay. *Bioconjugate Chemistry*, *22*(2), 289-298. http://dx.doi.org/10.1021/bc100421g

Popielec, A., & Loftsson, T. (2017). Effects of cyclodextrins on the chemical stability of drugs. *International Journal of Pharmaceutics*, *531*(2), 532-542. http://dx.doi.org/10.1016/j.ijpharm.2017.06.009

Pregosin, P. S., Kumar, P. G. A., & Fernandez, I. (2005). Pulsed Gradient Spin−Echo (PGSE) Diffusion and $^{1}H,^{19}F$ Heteronuclear Overhauser Spectroscopy (HOESY) NMR Methods in Inorganic and Organometallic Chemistry: Something Old and Something New. *Chemical Reviews*, *105*(8), 2977-2998. htpp://dx.doi.org/10.1021/cr0406716

Reina, J. J., Di Maio, A., Ramos-Soriano, J., Figueiredo, R. C., & Rojo, J. (2016). Rapid and efficient synthesis of α(1–2)mannobiosides. *Organic & Biomolecular Chemistry*, *14*(10), 2873-2882. http://dx.doi.org/10.1039/c6ob00083e

Riccio, D. A., & Schoenfish, M. H. (2012). Nitric oxide release: part I. Macromolecular scaffolds. *Chemical Society Review*, *41*(10), 3731-3741. http://dx.doi.org/10.1039/c2cs15272j

Schuster, J, Vijayakrishnan, B., & Davis, B. G. (2015). Chain-growth polyglycosylation: synthesis of linker equipped mannosyl oligomers. *Carbohydrate Research*, *403*(11), 135-141. http://dx.doi.org/10.1016/j.carres.2014.06.021

Seabra, A. B., & Durán, N. (2010). Nitric oxide-releasing vehicles for biomedical applications. *Journal of Materials Chemistry*, *20*(9), 1624-1637. http://dx.doi.org/10.1039/b912493b

Sortino, S., Giuffrida, S, De Guidi, G., Chillemi, R., Petralia, S., Marconi, G, et al. (2001). The photochemistry of flutamide and its inclusion complex with β-cyclodextrin. Dramatic effect of the microenvironment on the nature and on the efficiency of the photodegradation pathways. *Photochemistry and Photobiology*, *73*(1), 6-13. http://dx.doi.org/10.1562/0031-8655(2001)0730006tpofai2.0.co2

Sortino, S., Marconi, G., & Condorelli G. (2001). New insight on the photoreactivity of the phototoxic anti-cancer flutamide: photochemical pathways selectively locked and unlocked by structural changes upon drug compartmentalization in phospholipid bilayer vesicles. *Chemical Communication*, *2001*(13), 1226-1227. http://dx.doi.org/ 10.1039/b102359b

Szakács, G., Paterson, J. K. , Ludwig, J. A., Booth-Gent, C., & Gottesman, M. M. (2006). Targeting multidrug resistance in cancer. *Nature Reviews Drug Discovery*, *5*(3), 219-234. http://dx.doi.org/10.1038/nrd1984

Taladriz-Blanco P., & de Oliveira, M. G. (2014). Enhanced photochemical nitric oxide release from a flutamidederivative incorporated in Pluronic F127 micelles. *Journal of Photochemistry and Photobiology A: Chemistry*, *293*, 65-71. http://dx.doi.org/10.1016/j.jphotochem.2014.07.022

Taraszewska, J., Migut, K., & Koźbiał, M. (2003). Complexation of flutamide by native and modified cyclodextrins. *Journal of Physical Organic Chemistry*, *16*(2), 121-126. http://dx.doi.org/10.1002/poc.582

Taubes, G. (2008). The bacteria fight back. *Science*, *321*(5887), 356-361. http://dx.doi.org/10.1126/science.321.5887.356

van der Peet, P., Gannon, C. T., Walker, I., Dinev, Z., Angelin, M., Tam, S., et al. (2006). Use of click chemistry to define the substrate specificity of *Leishmania* β-1,2-mannosyltransferases. *ChemBioChem, 7*(9), 1384-1391. http://dx.doi.org/ 10.1002/cbic.200600159

Vargas-Berenguel, A., Ortega-Caballero, F., & Casas-Solvas, J. M. (2007). Supramolecular chemistry of carbohydrate clusters with cores having guest binding abilities. Mini-Reviews in Organic Chemistry, 4(1), 1-14. http://dx.doi.org/10.2174/157019307779815901

Wang, P. G., Cai, T. B., & Taniguchi, N. (Eds.) (2005). *Nitric Oxide Donors for Pharmaceutical and Biological Applications*. Weinheim: Wiley-VCH Verlag GmbH & Co. KGaA. http:/dx.doi.org/10.1002/3527603751

Wang, P. G., Xian, M., Tang, X., Wu, X., Wen, Z., Cai, T., et al. (2002). Nitric oxide donors: chemical activities and biological applications. *Chemical Reviews, 102*(4), 1091-1134. http://dx.doi.org/10.1021/cr000040l

Woodford, N., (2005). Novel agents for the treatment of resistant Gram-positive infections. *Expert Opinion on Investigational Drugs, 12*(2), 117-137. http://dx.doi.org/10.1517/13543784.12.2.117

Zhao, J., Liu, Y., Park, H.-J., Boggs, J. M., & Basu, A. (2012). Carbohydrate-coated fluorescent silica nanoparticles as probes for the galactose/3-sulfogalactose carbohydrate-carbohydrate interaction using model systems and cellular binding studies. *Bioconjugate Chemistry, 23*(6), 1166-1173. http://dx.doi.org/10.1021/bc2006169